Geochemistry Geophysics Geosystems G3
AN ELECTRONIC JOURNAL OF THE EARTH SCIENCES
PUBLISHED BY AGU AND THE GEOCHEMICAL SOCIETY

Article
Volume 1
May 30, 2000
Paper number 1999GC000032
ISSN: 1525-2027

Primitive CaO-rich, silica-undersaturated melts in island arcs: Evidence for the involvement of clinopyroxene-rich lithologies in the petrogenesis of arc magmas

P. Schiano
Department des Sciences de la Terre (UMR 6524), Université Blaise-Pascal, 5 rue Kessler, 63038 Clermont-Ferrand cedex, France (schiano@opgc.univ-bpclermont.fr)
Division of Geological and Planetary Sciences (170-25), California Institute of Technology, Pasadena, California 91125

J. M. Eiler
Division of Geological and Planetary Sciences (170-25), California Institute of Technology, Pasadena, California 91125 (eiler@gps.caltech.edu)

I. D. Hutcheon
Analytical and Nuclear Chemistry Division, Lawrence Livermore National Laboratory, P.O. Box 808, Livermore, California 94551 (hutcheon@llnl.gov)

E. M. Stolper
Division of Geological and Planetary Sciences (170-25), California Institute of Technology, Pasadena, California 91125 (ems@gps.caltech.edu)

[1] **Abstract:** On the basis of the study of olivine-hosted melt inclusions in a calc-alkaline basalt from Batan Island (Philippines) we define a distinctive type of primitive, nepheline-normative island arc magma characterized by unusually high CaO contents (up to 19.0 wt %) that cannot be simply explained by melting of the metasomatized peridotitic mantle wedge above subducting oceanic lithosphere. CaO-rich melt inclusions with these characteristics are preserved in Fo_{85-90} olivine, and compositional variations among the inclusions are interpreted to reflect mixing between melts such as those found in the most CaO-rich inclusions (present in Fo_{90} olivine) and melts similar to primitive "normal" island arc magmas (trapped in Fo_{85} olivine). Compilation of primitive island arc magmas from the literature shows that whole rocks and olivine-hosted melt inclusions with CaO contents >13 wt % are found in many arc volcanoes from all over the world in addition to Batan. These inclusions occur in lavas ranging from CaO-rich ankaramites to basaltic andesites with low-CaO contents (i.e., <13 wt %). The globally occurring CaO-rich inclusions and whole rocks comprise a group that although defined on the basis of their CaO contents is compositionally distinctive when compared to island arc lavas that have lower CaO contents; for example, they have lower FeO at a given SiO_2 content than most arc lavas, and they are all nepheline normative, with normative nepheline contents positively correlated with CaO contents. Variations in CaO content and normative compositions of experimental partial melts of lherzolite related to changes of pressure, temperature, and source composition suggest that there are no conditions under which partial melting of peridotite can generate melts having CaO contents and other properties comparable to those observed for the primitive, CaO-rich arc-derived melts identified here. Although melting of peridotite at high pressure in the presence of CO_2 can produce CaO-rich, silica-poor liquids,

we consider it unlikely that this is responsible for producing the CaO-rich, silica-undersaturated melts considered in this study because there are significant differences in nearly all other compositional characteristics between the CaO-rich arc magmas and melts known or thought to be produced by melting of carbonated peridotite. Model major element compositions of partial melts of clinopyroxene-rich lithologies (mantle pyroxenites, lower crustal pyroxenites, and eclogites) calculated using the MELTS algorithm suggest that the most CaO-rich, nepheline-normative melt inclusions and whole rocks identified here could represent intermediate to high degree (~10–40 wt %) partial melts of pyroxenites at lower crustal to upper mantle pressures. Such a hypothesis is supported by the comparison between the trace element compositions of model pyroxenite sources of the Batan CaO-rich melt inclusions and naturally occurring pyroxenites. The most likely source of the primitive CaO-rich, silica-undersaturated arc melts identified here is lower crustal and shallow upper mantle pyroxene-rich cumulates from arc environments because these cumulates have CaO concentrations at the upper end of the range observed for mantle pyroxenites. They are therefore more likely to yield partial melts with the restricted range of remarkably high CaO contents of the most CaO-rich inclusions and whole rocks identified here. Moreover, these cumulates often contain amphibole, which would lower their solidus temperatures relative to the anhydrous pyroxenite equivalents to values more consistent with those expected in deep crustal or shallow subarc environments.

Keywords: Melt inclusions; arc lavas.

Index terms: Chemical evolution; geochemical cycles; major element composition.

Received November 16, 1999; **Revised** March 9, 2000; **Accepted** March 15, 2000; **Published** May 30, 2000.

Schiano, P., J. M. Eiler, I. D. Hutcheon, and E. M. Stolper, 2000. Primitive CaO-rich, silica-undersaturated melts in island arcs: Evidence for the involvement of clinopyroxene-rich lithologies in the petrogenesis of arc magmas, *Geochem. Geophys. Geosyst.*, vol. 1, Paper number 1999GC000032 [15,276 words, 11 figures, 2 tables]. May 30, 2000.

1. Introduction

[2]K Most island arc lavas are believed to be derived from magmas formed by partial melting of the mantle overlying subducting oceanic lithosphere, where melting is fluxed by metasomatic enrichment in water (and other elements) carried by aqueous fluids and/or silicate melts released from the subducted oceanic crust [e.g., *Nicholls and Ringwood*, 1973]. The mantle sources on which this coupled enrichment-melting process operates are thought to be peridotites similar to or somewhat more depleted than the sources of mid-ocean ridge basalts (MORBs) [*Tatsumi et al.*, 1986; *Davidson*, 1987; *Nohda and Wasserburg*, 1981; *Ryerson and Watson*, 1987]. The trace element characteristics of arc lavas e.g., their high concentrations of large-ion lithophile elements (LILE) and their relatively low concentrations of high-field strength elements (HFSE)) and their major element compositions are influenced by the metasomatism, and high thermodynamic activities of H_2O strongly affect the compositions of primary magmas and their subsequent differentiation sequences [see *Stolper and Newman*, 1994, and references therein].

[3]K Although coupled metasomatism and fluxed melting of peridotites in the mantle wedge is believed to be the dominant process by which primary arc magmas form, some arc magmas have also been proposed to form by

melting of nonperidotitic sources: for example, partial melting of subducted crust [*Defant and Drummond*, 1990; *Drummond and Defant*, 1990; *Kay*, 1978], melting at deep crustal levels [*Pichler and Zeil*, 1972], and melting of an ocean island basalt-type source [*Ito and Stern*, 1985] have all been proposed. In this article, we document a distinctive type of primitive, nepheline-normative island arc magma characterized by unusually high CaO contents (up to 19 wt %) that cannot be simply reconciled with the standard model of arc petrogenesis described above. Although arc-derived samples with these characteristics have been previously reported [*Metrich et al*., 1999; *Sisson and Bronto*, 1998; *Della-Pasqua and Varne*, 1997; *Gioncada et al*., 1998; *Metrich and Clocchiatti*, 1996; *Foden and Varne*, 1980; *Foden*, 1983; *Kennedy et al*., 1990; *Carr and Rose*, 1984; *Thirwall and Graham*, 1984; *Shimizu and Arculus*, 1975; *Arculus*, 1976], they have not been recognized as a coherent, globally occurring magma type or as distinct from CaO-rich magmas found in oceanic island [*Tronnes*, 1990], mid-ocean ridge [*Kamenetsky et al*., 1998; *Sours-Page et al*., 1999], and back arc [*Kamenetsky et al*., 1997] settings. After documenting the existence of this distinctive magma type, emphasizing in particular a well-defined group from Batan Island (northernmost Philippines, Luzon-Taiwan arc), but also showing that such magmas occur in arcs from around the world, we examine the compositions of CaO-rich, silica-undersaturated magmas in subduction zone settings with the following objectives in mind: (1) to provide a compilation of the occurrences and compositions of such magmas; (2) to examine their relationship to more typical magmas in subduction zone settings; (3) to estimate plausible chemical and mineralogical characteristics of their sources; and (4) to evaluate the implications of their existence for models of melt generation in subduction zones.

2. Definition of a Distinctive CaO-Rich, Silica-Undersaturated Magma Type From Subduction Zone Settings

2.1. CaO-Rich, Silica-Undersaturated Melt Inclusions in Olivine Phenocrysts in Lavas From Batan Island (Northernmost Philippines, Luzon-Taiwan Arc)

2.1.1. Sample description, analytical techniques, and results

[4] The geologic setting of Batan Island and the petrography of its principal rock types (basalts, basaltic andesites, and andesites) are described by *Richard et al*. [1986]. Plagioclase, olivine, and clinopyroxene dominate the phenocryst assemblages of the basalts, while basic and acid andesites contain phenocrysts of clinopyroxene, hornblende, plagioclase, and titanomagnetite. Sample B45 from Mount Iraya, the youngest (2.32 to <0.1 myr) volcano on Batan Island [*Richard et al*., 1986], is a high-MgO (10.8 wt %) calc-alkaline basalt [*Metrich et al*., 1999; *Richard et al*., 1986]. Compositions of primary melt inclusions in olivine phenocrysts (Fo_{90-75}) from this sample were determined on glasses produced after heating each inclusion up to its homogenization temperature (i.e., the temperature at which the inclusion contents (gas, glass, and crystals) homogenized visually to a uniform melt phase). Heating experiments were performed with a high-temperature, optical heating-stage apparatus [*Sobolev et al*., 1980] that allowed visual monitoring of individual melt inclusions during heating. Homogenization temperatures were 1220 ± 20°C, and effective times of quenching were <1 s. Comparison between the compositions of homogenized and unheated glass inclusions trapped in olivine phenocrysts with similar forsterite content shows that the amount of host olivine needed to be added to the unheated glass inclusions to get the heated ones is relatively

small (≤15% in weight). Consequently, the effect of the heating procedure on the concentrations of elements other than MgO (and to a lesser extent FeO and SiO_2) is relatively small, and therefore the main conclusions of the paper would be unchanged if unheated inclusions were considered. It should be noted that this statement applies not only to the Batan samples but also to those in the compilation that will be presented later in this article.

Table 1. Representative Major and Trace Element Compositions of Homogenized Melt Inclusions in Olivine in a Calc-Alkaline Basalt (B45) From Batan Island (20°25′N–121°54′E, Luzon-Taiwan Arc)[a]

	Sample Identification								
	B7-1	B7-2	B2-1	B4	B1-2	B1-1	B5-1	B8-1	B6-1
SiO_2, wt %	44.02	45.05	44.00	45.61	44.10	44.04	45.89	49.42	54.73
TiO_2, wt %	0.70	0.64	0.79	0.67	0.94	0.76	0.74	0.91	0.98
Al_2O_3, wt %	16.01	16.87	14.92	16.58	16.13	16.02	16.43	15.39	14.44
FeO*, wt %	7.31	6.80	8.86	8.02	8.82	8.85	12.27	11.11	8.84
MnO, wt %	0.12	0.10	0.15	0.14	0.14	0.15	0.20	0.18	0.19
MgO, wt %	8.30	8.27	8.96	8.36	7.67	7.72	6.71	7.17	5.63
CaO, wt %	18.54	17.08	17.20	16.27	17.20	17.06	11.57	10.22	7.48
Na_2O, wt %	2.58	2.56	2.43	2.53	2.29	2.60	2.75	3.05	3.29
K_2O, wt %	0.93	1.01	0.86	1.01	0.90	1.01	1.40	1.43	2.17
Cr_2O_3, wt %	0.05	0.04	0.05	0.08	0.04	0.03	0.08	0.08	0.03
SUM	98.57	98.42	98.20	99.26	98.23	98.24	98.02	98.95	97.77
HOST	Fo_{89}	Fo_{89}	Fo_{89}	Fo_{87}	Fo_{86}	Fo_{86}	Fo_{78}	Fo_{79}	Fo_{78}
Ba, ppm	219	214	185	237	136	245	215	323	423
Th, ppm	2.12	2.18	1.57	2.32	1.04	2.87	2.06	3.74	6.75
U, ppm	0.63	0.57	0.38	0.49	0.31	0.67	0.39	0.91	1.37
Nb, ppm	2.20	2.26	4.40	2.35	2.09	2.83	2.68	4.00	6.17
Sr, ppm	537	539	498	490	398	571	536	663	561
Zr, ppm	56.1	60.7	52.6	58.6	47.0	66.9	62.7	90.2	124.7
Y, ppm	17.3	17.0	19.9	14.1	13.4	17.1	17.9	26.7	25.2
Sc, ppm	53	44	62	43	56	48	N.D.	N.D.	26
La, ppm	9.21	9.39	8.31	9.10	7.45	10.52	9.11	13.13	18.40
Ce, ppm	21.4	20.9	18.4	21.2	15.7	24.9	19.8	31.5	43.3
Nd, ppm	14.3	14.2	12.3	13.6	10.7	19.3	13.2	22.4	26.2
Sm, ppm	3.15	2.99	2.61	3.00	1.95	3.49	2.86	4.33	4.99
Eu, ppm	0.95	0.92	0.67	0.85	0.57	0.99	0.83	1.30	1.26
Dy, ppm	2.81	2.95	2.47	2.58	1.94	3.01	2.46	4.56	4.56
Er, ppm	2.09	2.01	1.85	1.82	1.21	2.07	1.93	3.42	3.32
Yb, ppm	2.34	2.26	2.26	2.09	1.39	2.31	2.25	3.77	3.37

[a]Major element compositions were measured with the Caltech 5-spectrometer JEOL 733 microprobe using an accelerating voltage of 15 Kv, a sample current of 10 nA and a defocused beam (size ~20 μm). Data were reduced using a modified ZAF procedure (CITZAF [*Armstrong*, 1988]). The reproducibility and accuracy of the Na measurements were tested on glass standards. The abundances of Sr, Y, Zr, Nb, Ba, rare earth elements, Th, and U were determined with the Lawrence Livermore National Laboratory (LLNL) ion microprobe, a modified Cameca IMS-3f instrument, using a 17 keV, $^{16}O^-$ primary ion beam, focused into a ~20-μm-diameter spot. Positive secondary ions were extracted and accelerated, nominally to 4500 V. A field aperture inserted in the sample image plane allowed only ions from the central 30-μm-diameter area of the imaged field to enter the mass spectrometer. Isobaric molecular interferences were minimized by energy filtering, using a 40-eV window and offsetting the accelerating voltage by 100 V from the voltage at which the energy distribution of $^{16}O^+$ dropped to 10% of its maximum value. Trace element concentrations were determined from ^{42}Ca-normalized ion intensities using sensitivity factors established from analyses of a suite of silicate glass and mineral standards. Each analysis consisted of 8–10 cycles over the masses of interest. On the basis of analyses of NIST glass standards (NBS-610, -612, and -614, using the concentrations given by *Pearce et al*. [1997], the accuracy varies between ±3 and ±10% for Sr, Y, Zr, Ba, La, Ce, Nd, Er, and Yb, between ±10 and ±15% for Nb, Th, Sm, and Dy, and between ±15 and ±25% for U and Eu. Sc analyses were carried out at a mass resolving power of 4000 and zero energy offset, using a 2-nA $^{16}O^-$ primary ion beam. The ^{42}Ca-normalized ion intensities were converted to concentrations using sensitivity factors established from analyses of NIST standard glass SRM 612.

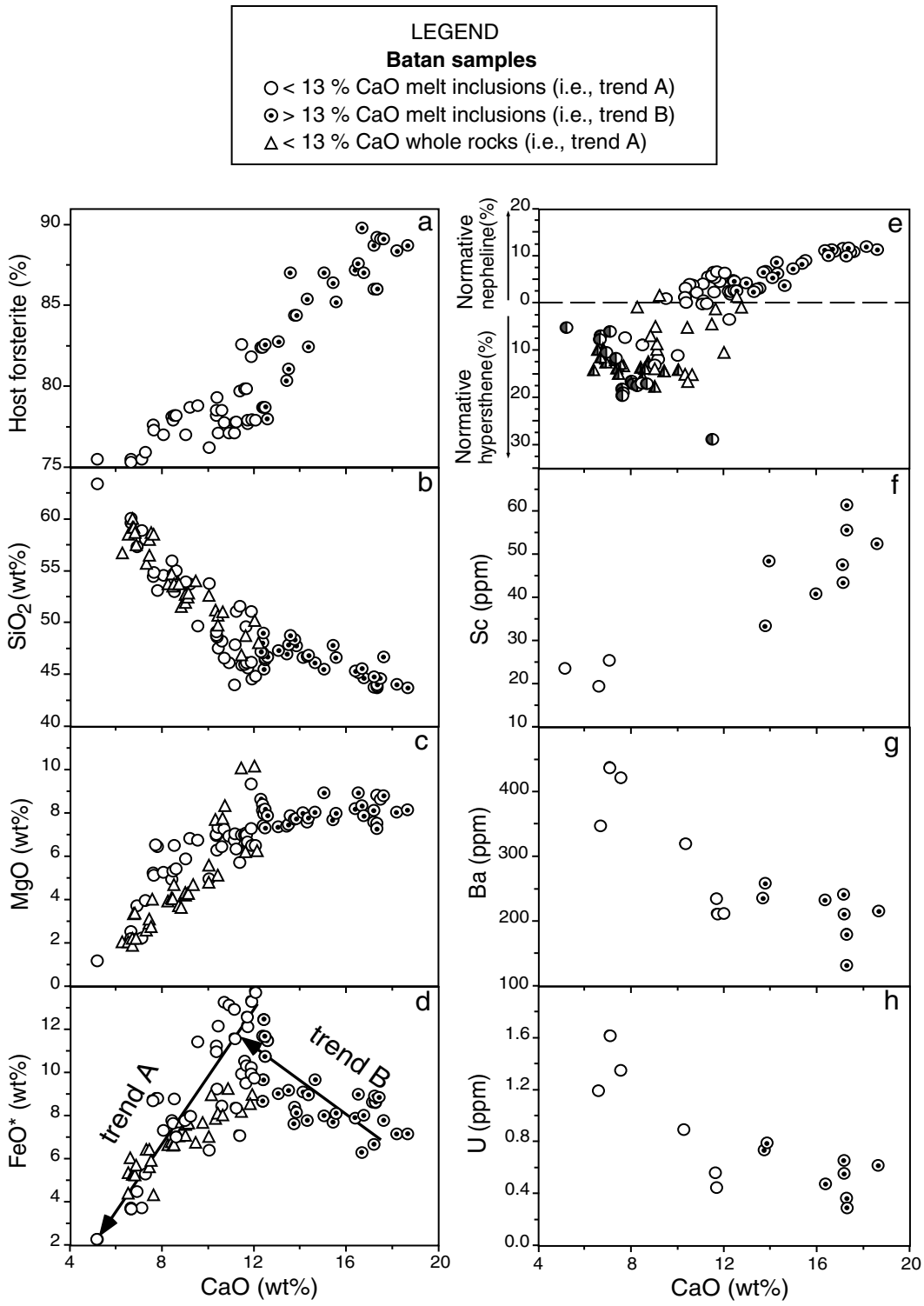
LEGEND
Batan samples
< 13 % CaO melt inclusions (i.e., trend A)
> 13 % CaO melt inclusions (i.e., trend B)
< 13 % CaO whole rocks (i.e., trend A)
a
b
c
d
e
f
g
h
Host forsterite (%)
SiO2 (wt%)
MgO (wt%)
FeO* (wt%)
Normative nepheline(%)
Normative hypersthene(%)
Sc (ppm)
Ba (ppm)
U (ppm)
trend A
trend B
CaO (wt%)
CaO (wt%)

[5] Homogenized inclusions were analyzed for major and minor elements using the electron microprobe at Caltech and for trace elements (Sc, Sr, Y, Zr, Nb, Ba, rare earth elements (REE), Th, and U) using the ion microprobe at the Lawrence Livermore National Laboratory (Table 1; see footnote for analytical procedures). The inclusions range in composition from nepheline-normative basalt to quartz-normative dacite; major element variations in these glasses are illustrated in Figure 1. The CaO and MgO contents decrease from 18.5 to 5.0 wt % and 9.5 to 1.3 wt %, respectively, as SiO_2 increases from 44.3 to 63.7 wt %. Variations in the compositions of melt inclusions are well correlated with the Mg# of their host olivines, with the most SiO_2-poor and CaO- and MgO-rich inclusions trapped in the most magnesian olivines ($\sim Fo_{90}$) and the most SiO_2-rich and CaO- and MgO-poor inclusions trapped in the least magnesian olivines ($\sim Fo_{75}$).

[6] Trace element compositions of olivine-hosted melt inclusions are also well correlated with major element composition: for example, Sc content decreases from 65 to 20 ppm and incompatible trace elements increase regularly as CaO decreases (Figures 1f–1h). The mid-ocean ridge basalt (MORB)-normalized trace element patterns of the inclusions (Figure 2a) are typical of arc magmas (i.e., enriched in LILE and depleted in HFSE and in high REE (HREE) relative to MORB; enriched in low REE (LREE) relative to HREE); these trace element features are thought to reflect melting of mantle sources depleted with respect to the sources of MORB that have been metasomatized by a slab-derived, H_2O-rich component [*Stolper and Newman*, 1994]. Note that although the incompatible element concentration variations are correlated with major element composition, the La/Yb ratio does not increase as the CaO content decreases (Figure 2a).

[7] Although in most variation diagrams the melt inclusions and previously analyzed whole rocks from Batan [*Richard et al.*, 1986; *Maury et al.*, 1998; *McDermott et al.*, 1993] define a single trend, with the CaO-rich inclusions falling on a continuous extension of the trend defined by the inclusions with lower CaO contents, Figure 1d shows that this is not the case for FeO: that is, the CaO-rich inclusions define a population offset toward lower FeO contents from the trend of whole rocks and lower-CaO inclusions. For the purposes of later discussion, we refer to the trend defined by the Batan whole rocks and lower-CaO inclusions as trend A and the higher CaO, lower FeO trend as trend B. Note that inclusions from trends A and B do not occur in the same olivine phenocrysts. The distinction between trends A and B is also illustrated in Figure 3, in which the compositions of the melt inclusions and Batan whole rocks were first recalculated to equivalent CaO-MgO-Al_2O_3-SiO_2 (C-M-A-S) [*O'Hara*, 1968; *Basaltic Volcanism Study Project*, 1981] and then projected from alumina onto the S-C-M plane. Also shown on this diagram are experimentally determined trends for olivine + clin-

Figure 1. CaO variation diagrams comparing melt inclusions (circles) in olivine phenocrysts from B45 basalt from Batan Island (Luzon-Taiwan arc) (this study and *Metrich et al.* [1999]) with Batan whole rocks (triangles) [*Richard et al.*, 1986; *Maury et al.*, 1998; *McDermott et al.*, 1993]. Trend A (open symbols) comprises low-CaO melt inclusions and all Batan whole rocks and is interpreted as due to progressive fractionation of olivine + clinopyroxene + amphibole (see Figure 3); trend B (dotted circles) comprises the CaO-rich inclusions and is interpreted as due to magma mixing between liquids similar to the most CaO-rich inclusions in trend B (i.e., in the Fo_{90} olivines) and melts near the most primitive end of trend A. Normative compositions are calculated assuming $Fe^{3+} = 0.15 \sum Fe$. Half-solid circles and triangles in Figure 1e are quartz normative samples.

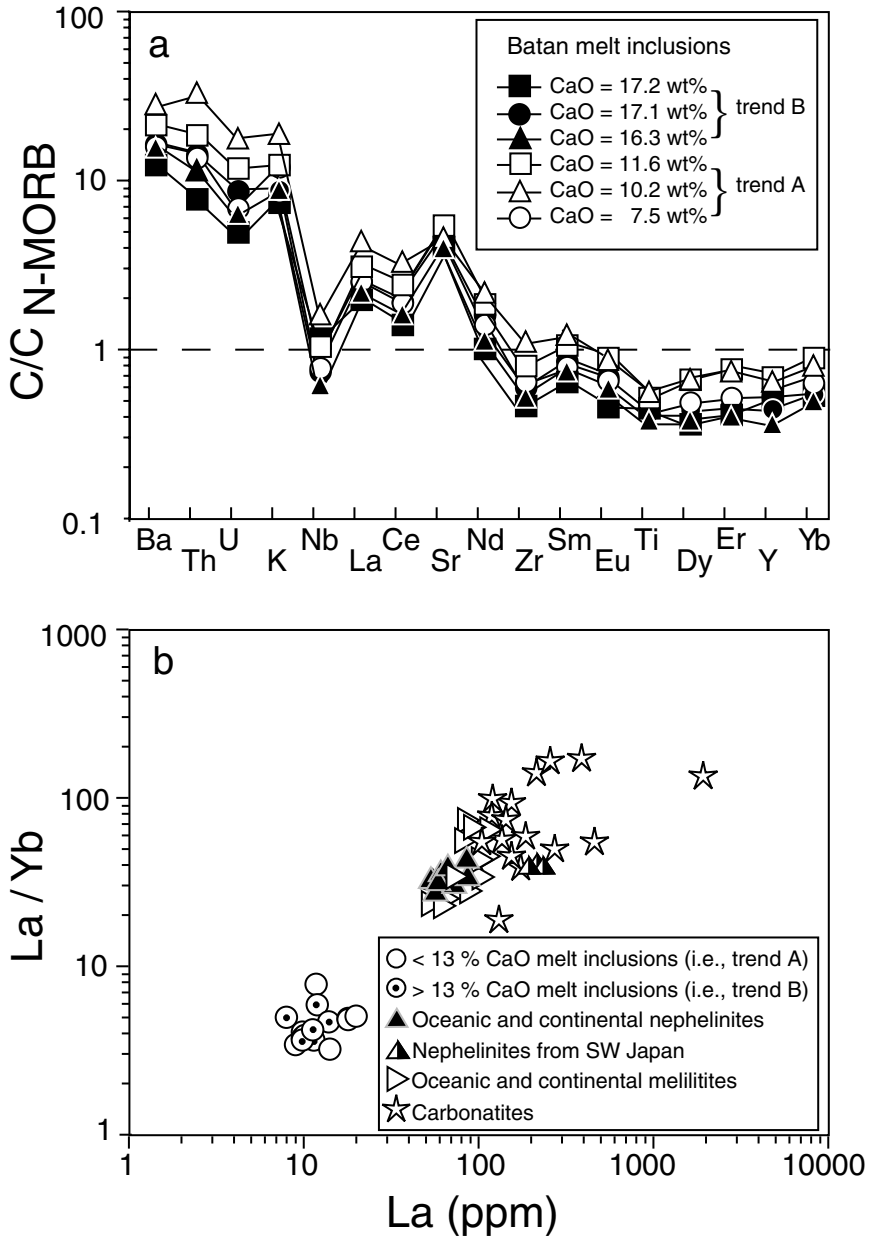

Figure 2. (a) Normal mid-ocean ridge basalt (NMORB)-normalized diagram showing trace element data for melt inclusions in olivine phenocrysts in B45 basalt from Batan Island. The order of elements is based on the incompatibility sequence during MORB petrogenesis [*Hofmann*, 1988]. Compositions are normalized to the average NMORB composition of *Hofmann* [1988]. (b) Plot of La/Yb ratio versus La concentration comparing data for Batan melt inclusions with data for primitive melilitites [*Wilson et al*., 1995], nephelinites from oceanic and continental regions [*Wedephol et al*., 1994; *Hoernle and Schmincke*, 1993], nephelinites from SW Japan [*Tatsumi et al*., 1999], and carbonatites from Africa, Australia, Europe, and North and South America [*Nelson et al*., 1988]. Symbols are given in the accompanying legend, and the distinction between trend A and trend B for the Batan samples is the same as in Figure 1.

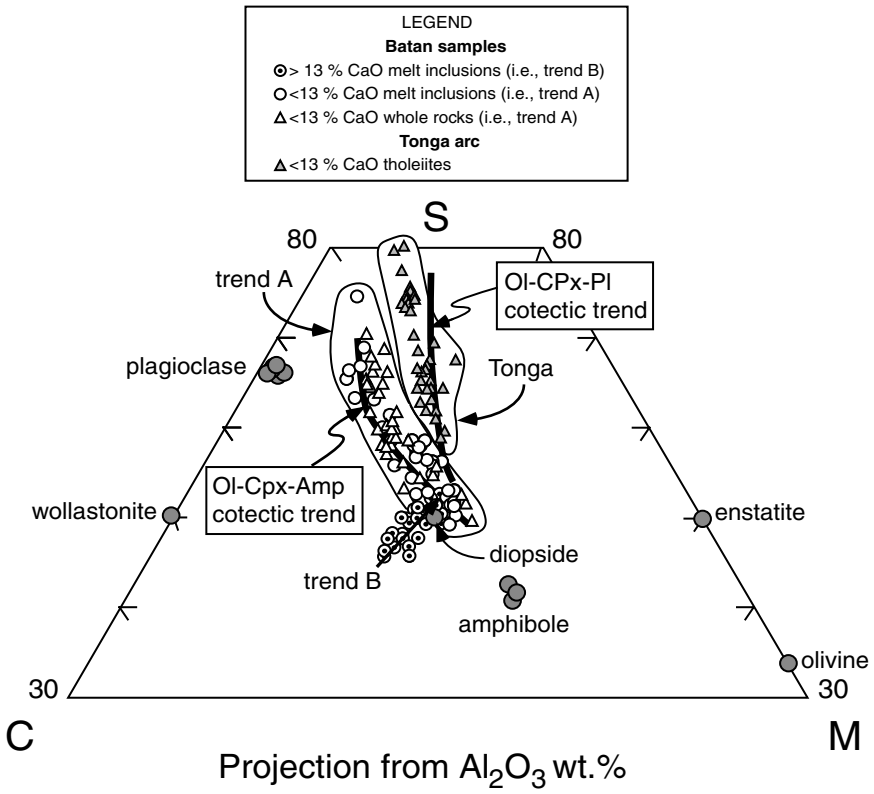

Figure 3. Compositions of Batan melt inclusions (circles) and whole rocks (triangles) recalculated to equivalent CaO-MgO-Al_2O_3-SiO_2 (C-M-A-S) and then projected from alumina onto the S-C-M plane. The distinction between trend A (open symbols) and trend B (dotted circles) for the Batan samples is the same as in Figure 1. Also shown on this diagram are experimentally determined trends for olivine-clinopyroxene-plagioclase-saturated melts at 1 atm and olivine-clinopyroxene-amphibole-saturated liquids at 2 kbar (H_2O-saturated) [*Tormey et al.*, 1987; *Grove and Bryan*, 1983; *Walker et al.*, 1979; *Grove et al.*, 1982; *Cawthorn and O'Hara*, 1976; *Sisson and Grove*, 1993] and the trend of whole rocks (shaded triangles) from the Tonga arc (SW Pacific), a typical tholeiitic arc series [*Ewart et al.*, 1973, 1977; *Gill*, 1981]. Plagioclase and amphibole compositions are from [*Tormey et al.*, 1987; *Grove and Bryan*, 1983; *Walker et al.*, 1979; *Grove et al.*, 1982; *Cawthorn and O'Hara*, 1976; *Sisson and Grove*, 1993]. Analyses have been recalculated as CMAS components by following a modified version [*Basaltic Volcanism Study Project*, 1981] of the procedure used by *O'Hara* [1968]. The procedure is as follows: C = (CaO − P_2O_5/3 + K_2O + $2Na_2O$)56.08; A = (Al_2O_3 + Cr_2O_3 + Fe_2O_3 + Na_2O)101.96; M = (MgO + FeO + MnO)40.30; S = (SiO_2 − $2Na_2O$ − $4K_2O$)60.08. All oxides are in molecular proportions.

opyroxene + plagioclase-saturated liquids at 1 atm and olivine + clinopyroxene + amphibole-saturated liquids at 2 kbar (H_2O saturated) [*Tormey et al.*, 1987; *Grove and Bryan*, 1983; *Walker et al.*, 1979; *Grove et al.*, 1982; *Cawthorn and O'Hara*, 1976; *Sisson and Grove*, 1993] and the trend of whole rocks from the Tonga arc (SW Pacific), a typical tholeiitic arc series [*Ewart et al.*, 1973, 1977; *Gill*, 1981].

2.1.2. Compositional evolution of Batan melt inclusions

[8] The observation that the most CaO-rich and SiO_2-poor melts are trapped in the most for-

steritic olivine crystals (Figure 1a) suggests that the CaO-rich, silica-undersaturated melts are relatively primitive. In this section, we evaluate the origin of the compositional variation from this primitive end of the array of melt inclusion compositions to the CaO-poor, SiO_2-rich compositions contained in the least forsteritic olivines.

[9] One possible explanation for the relationship between melt inclusion composition and the Mg# of the host olivine is that compositional variations in melt inclusions represent a trend of fractional crystallization. However, although the correlated decreases in the Mg# of the host olivines and the MgO and CaO contents of the inclusions would be consistent with fractional crystallization of a clinopyroxene ± olivine-bearing assemblage, such a fractionating assemblage (assuming the clinopyroxene to be compositionally similar to the diopside, augite, or salite phenocrysts in Batan lavas [*Richard et al.*, 1986]) could not readily account for the decrease in normative nepheline with decreasing CaO content shown in Figure 1e (i.e., crystallization of such an assemblage from nepheline-normative liquids typically results in increasing rather than decreasing normative nepheline [*Sack et al.*, 1987]). Likewise, although fractional crystallization of assemblages dominated by nepheline-normative minerals such as amphibole, jadeite, or acmite could, in principle, decrease the normative nepheline contents of residual liquids, it would not decrease their CaO contents.

[10] Figures 1b–1d show that trend A (defined by melt inclusions) is typical of the compositional trend of whole rock analyses of lavas from Batan (shown as triangles in Figure 1). As indicated above, Figure 1d also demonstrates the important point that trend B, defined by the CaO-rich inclusions, is not simply an extension or continuation of the compositional trends of arc lavas from Batan; this point is also made in Figure 3, where the CaO-poor melt inclusions and whole rocks defining trend A follow the olivine-clinopyroxene-amphibole cotectic but the trend B melt inclusions fall off this cotectic. The correspondence of trend A to the olivine-clinopyroxene-amphibole cotectic suggests that the compositional variations of Batan whole rocks could primarily reflect relatively low pressure crystallization of an amphibole-bearing assemblage from low-CaO, high-FeO parental melts comparable to those with ~12 wt % CaO trapped in Fo_{85} olivine. This consistency of major element variations in Batan lavas with fractional crystallization of an amphibole-bearing assemblage agrees with the conclusions of several previous studies [*Richard et al., 1986; Maury et al., 1988; McDermott et al.*, 1993]. Note that the tholeiitic trend of whole rock lavas from the Tonga arc shown in Figure 3 contrasts with the Batan trend and suggests the Tonga trend is produced by low-pressure fractionation of an olivine-clinopyroxene-plagioclase assemblage. This hypothesis is supported by mass balance calculations [see *Gill*, 1981, page 272] that indicate that fractionation of an olivine-clinopyroxene-plagioclase assemblage can account quantitatively for major element variation within the Tonga volcanic suite.

[11] We thus conclude that trend A, comprising the low-CaO Batan melt inclusions and the Batan whole rock lavas, can be interpreted relatively simply in terms of progressive extraction of olivine + clinopyroxene + amphibole from a parental basaltic liquid with ~12 wt % CaO and 8–10 wt % MgO, but that trend B cannot be explained as readily by crystallization differentiation. Likewise, progressive partial melting of a peridotitic source is unlikely to account for trend B, since this would produce a positive correlation between CaO and FeO if the source contains residual clinopyroxene [e.g., *Kinzler and Grove,* 1992a, b; *Baker and Stolper*, 1994; *Hirose and Kush-*

Table 2. Representative Major Element Compositions of the CaO-Rich, Silica-Undersaturated Melt Inclusions and Whole Rocks in Island Arcs Identified in This Study[a]

	Host	Arc	Volcano	Sample	SiO_2	TiO_2	Al_2O_3	FeO*	MnO	MgO	CaO	Na_2O	K_2O	P_2O_5	Cr_2O_3	Sum	Reference
Inclusion	Fo_{89}	Java	Galunggung	J-1	45.00	1.20	19.20	6.04	0.09	4.39	18.70	3.07	0.53	0.14	N.D.	98.45	S&B (98)
Inclusion	Fo_{88}			F-1	43.90	1.28	18.40	7.53	0.09	4.99	18.40	3.49	0.66	0.18	N.D.	99.03	S&B (98)
Inclusion	Fo_{84}			I-E	44.20	1.30	19.20	8.60	0.10	4.10	17.70	2.70	0.42	0.12	N.D.	98.57	S&B (98)
Inclusion	Fo_{94}	Vanuatu	Merelava	31551	46.20	0.49	13.68	8.87	0.09	12.47	15.53	1.55	0.56	0.41	N.D.	99.98	D&V (97)
Inclusion	Fo_{91}			31551	45.88	0.46	14.07	8.87	0.02	12.18	15.89	1.59	0.52	0.37	N.D.	99.98	D&V (97)
Inclusion	Fo_{91}	E. Sunda	Rindjani	48002	43.39	1.13	15.35	9.36	0.05	11.77	15.24	2.43	0.98	0.16	N.D.	100.00	D&V (97)
Inclusion	Fo_{90}			48001	45.49	0.93	14.23	8.57	0.14	9.54	17.76	1.85	1.33	0.16	N.D.	100.13	D&V (97)
Lava				48001	48.32	0.69	10.53	9.05	0.17	14.02	14.38	1.50	0.90	0.15	N.D.	99.85	F (83)
Inclusion	Fo_{90}	Eolian	Stromboli	ol5/b118	48.88	0.75	12.97	6.51	N.D.	8.16	13.78	1.85	1.59	0.32	N.D.	94.91	M&C (96)
Inclusion	Fo_{90}		Vulcano	IV88.1	44.46	0.55	11.69	7.82	0.15	8.50	15.58	2.63	3.67	0.43	0.05	95.65	G (98)
Inclusion	Fo_{90}			IV88.3.1	45.34	0.80	9.99	7.92	0.11	8.94	15.30	2.34	3.04	0.44	0.06	94.40	G (98)
Lava		N. Guinea	Lihir	L3	47.35	0.76	12.46	10.36	0.21	9.12	14.73	2.90	0.44	0.36	N.D.	98.85	K (90)
Lava				L6	47.24	0.90	12.69	10.37	0.21	7.47	13.12	2.15	2.23	0.49	N.D.	97.03	K (90)
Lava		Nicaragua	N.D.	CR-T	43.74	1.75	13.81	9.39	0.15	8.87	15.26	2.66	1.03	0.90	N.D.	97.70	C&R (84)
Lava		Lesser	Grenada	6155	46.93	0.97	16.16	9.39	0.17	7.57	14.53	1.82	1.01	0.20	N.D.	98.88	T&G (84)
Lava		Antilles		450	47.17	0.96	15.58	10.01	0.18	7.06	14.43	2.12	0.52	0.12	N.D.	98.31	T&G (84)
Lava				503	45.60	0.95	15.91	8.53	0.18	10.95	13.50	1.88	1.01	0.40	N.D.	99.04	S&A (75)
Inclusion	Fo_{89}	Luzon	Batan	B45/53	44.33	0.73	16.74	7.19	0.12	8.18	18.07	2.72	0.91	0.37	N.D.	99.91	M (98)
Inclusion	Fo_{89}			B45/43a	46.98	0.64	14.03	7.82	0.14	8.95	17.50	2.51	0.96	0.17	N.D.	100.14	M (98)
Inclusion	Fo_{89}			B45/43b	44.92	0.77	15.68	8.93	0.15	8.79	17.36	2.44	0.83	0.64	N.D.	101.05	M (98)

[a]FeO* is total iron reported as FeO. N.D., not determined. References: S&B (98), *Sisson and Bronto* [1998]; D&V (97), *Della-Pasqua and Varne* [1997]; F (83), *Foden* [1983]; M&C (96), *Metrich and Clocchiatti* [1996]; G (98), *Gioncada et al*. [1996]; K (90), *Kennedy et al*. [1990]; C&R (84), *Carr and Rose* [1984]; T&G (84), *Thirwall and Graham* [1984]; S&A (75), *Shimizu and Arculus* [1975]; M (98), *Metrich et al*. [1998].

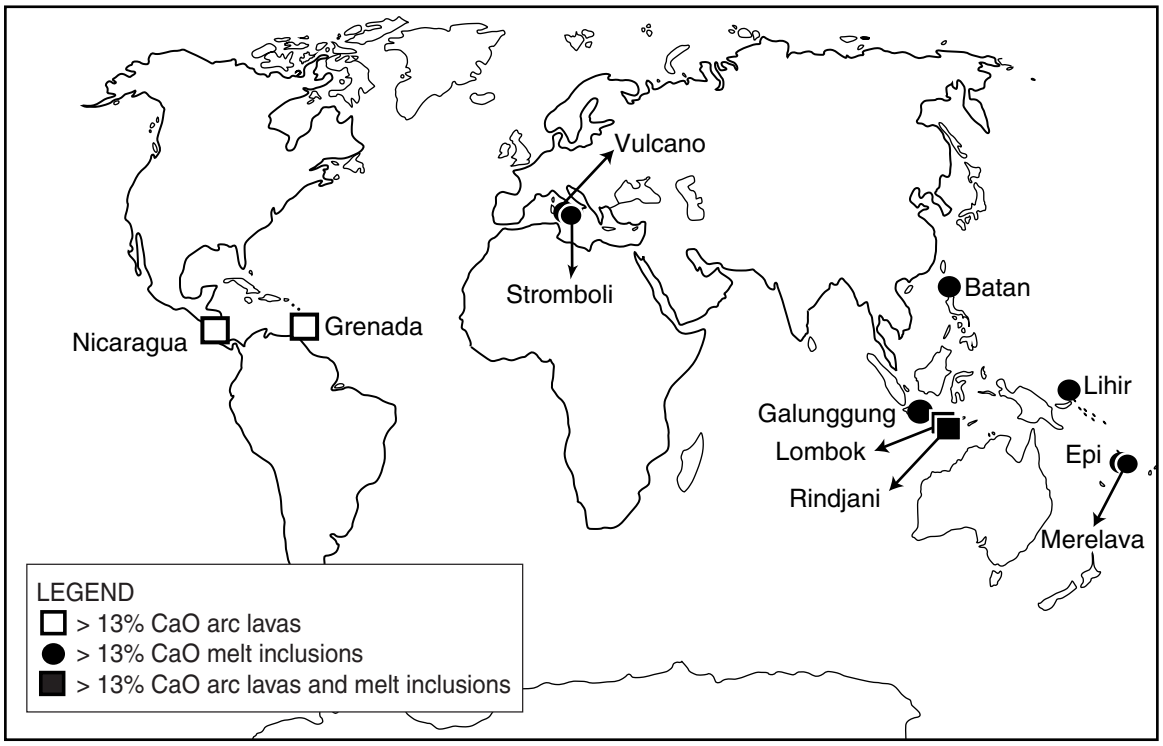

Figure 4. Map showing the locations of the CaO-rich, silica-undersaturated whole rocks and melt inclusions mentioned in the text. Solid circles indicate locations where CaO-rich inclusions have been found, open squares indicate locations where CaO-rich whole rocks have been found, and solid squares indicate locations where both have been found.

ino, 1993], contrary to what is observed for trend B (Figure 1d). Moreover, as discussed below (see section 4.1), trend B probably cannot be explained by progressive melting of a pyroxene-rich lithology at a constant pressure, because current estimates suggest that progressive melting of pyroxenite results in liquids with increasing CaO and decreasing normative nepheline, contrary to the observed trend.

[12] Our preferred explanation for the compositional variation among the CaO-rich inclusions (i.e., those defining trend B) is that it represents a mixing trend between the most CaO-rich inclusions (i.e., those in the Fo_{90} olivines) and melts near the most primitive end of the "normal" Batan trend that we have defined as trend A. Figures 1 and 3 demonstrate that this can indeed explain the trend B. Although it is difficult to test this explanation for trend B using only the chemical compositions of melt inclusions, in principle, isotopic differences between inclusions along the compositional array or detailed petrographic investigation of whole rocks on this trend could be used to evaluate this hypothesis.

2.2. Compilation of the Occurrences and Compositions of CaO-Rich, Silica-Undersaturated Melts in Subduction Zone Settings

[13] We compiled from the literature the compositions of arc-related whole rock samples

and olivine-hosted melt inclusions having CaO contents >13 wt % (Table 2). In addition to the Batan inclusions (this study and *Metrich et al.* [1999]), whole rocks and melt inclusions with CaO contents >13 wt % are found in volcanoes from many convergent margins (Figure 4), including Galunggung (Sunda arc), Stromboli and Vulcano (Aeolian arc), Lihir (New Guinea), Nicaragua (Central America), Grenada (Lesser Antilles), Lombok (Sunda arc), Rindjani (Sunda arc), and Epi and Merelava (Vanuatu arc) [*Sisson and Bronto*, 1998; *Della-Pasqua and Varne*, 1997; *Gioncada et al.*, 1998; *Metrich and Clocchiatti*, 1996; *Foden and Varne*, 1980; *Foden*, 1983; *Kennedy et al.*, 1990; *Carr and Rose*, 1984; *Thirwall and Graham*, 1984; *Shimizu and Arculus*, 1975; *Arculus*, 1976].

[14] All the inclusions reported in Table 2 are hosted by Mg-rich olivine (Fo_{84-94}) in basalts, basaltic andesites, or ankaramites. As was done for the Batan samples reported here, they were homogenized by high-T experiments to reverse postentrapment crystallization of the host crystal [*Roedder*, 1984; *Schiano and Bourdon*, 1999], with the exception of inclusions from Galunggung [*Sisson and Bronto*, 1998], which were instead corrected by oli-

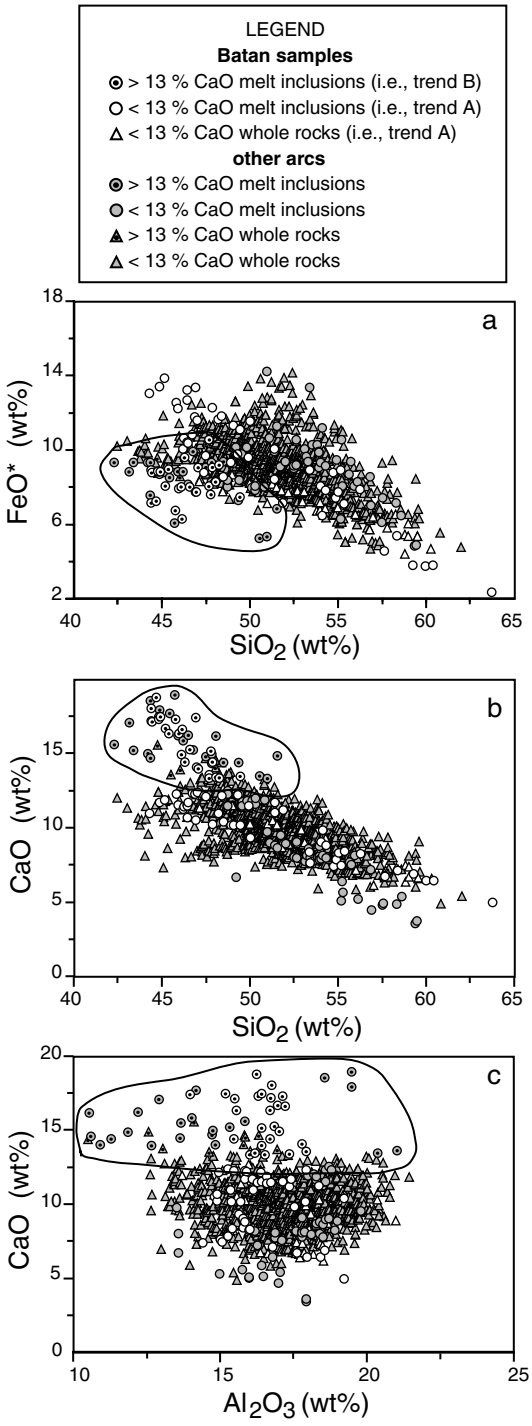

Figure 5. Variation diagrams comparing Batan CaO-rich melt inclusions (i.e., trend B) and CaO-rich melt inclusions and whole rocks from other arc environments (all of which have CaO > 13 wt %) with "normal" melt inclusions and whole rocks from Batan and other arcs (all of which have CaO contents < 13 wt %) (shaded triangles without dot, 1350 basalts with MgO > 4.5 wt % from 30 arcs, compiled by *Plank and Langmuir* [1988]. Shaded circles without dot, melt inclusions in olivine phenocrysts from *Gioncada et al.* [1998] and *Sisson and Layne* [1993]). Symbols are given in the accompanying legend. FeO* is total iron reported as FeO. Major element concentrations have been normalized to 100%.

vine addition (5–13% in weight [*Sisson and Bronto*, 1998]) to be in Fe-Mg equilibrium with the host olivine.

[15] The CaO-rich melt inclusions from arcs worldwide overlap the trend B inclusions from Batan in major element variation diagrams (Figure 5). They are also indistinguishable from CaO-rich whole rocks from arcs. On the other hand, the trend A inclusion and whole rocks from Batan overlap the compositional trend of CaO-poor whole rocks and melt inclusions from other arcs (Figure 5). Inspection of Figure 5 shows that as shown above on a local scale for the Batan samples, on a global scale these arc-derived CaO-rich compositions collectively form a group that although defined on the basis of their CaO contents is compositionally distinctive when compared to arc lavas and melt inclusions having lower CaO contents. The compositional characteristics of this group are the same as those of trend B melt inclusions from Batan described above: for example, CaO-rich inclusions and lavas are characterized by lower FeO concentrations at a given SiO_2 content than most arc lavas (Figure 5), and they are all nepheline normative (0.5–16.2% normative nepheline), with normative nepheline contents positively correlated with CaO contents (Figure 6). They thus differ from the CaO-rich compositions found as olivine-hosted melt inclusions and whole rocks in oceanic island [*Tronnes*, 1990], mid-ocean ridge [*Kamenetsky et al.*, 1998; *Sours-Page et al.*, 1999], and back arc [*Kamenetsky et al.*, 1997] settings, all of which are hypersthene normative (Figure 6). The CaO-rich inclusions and whole rocks also have highly variable CaO/Al_2O_3 ratios (0.8–1.4) and silica contents at the low end (44–48.5 wt %) of the distribution of arc lavas. The CaO-rich whole rocks are characterized by relatively high MgO (>6.5 wt %) contents, and although MgO contents of inclusions are sensitive to the correction for postentrapment crystallization, homogenized CaO-rich inclusions are also MgO-rich ($\geq$7.5 wt %). Note that although the whole rocks are clinopyroxene-phyric (diopside-augite [*Foden and Varne*, 1980; *Foden*, 1983; *Kennedy et al.*, 1990; *Thirwall and Graham*, 1984]), their elevated CaO contents and silica undersaturation cannot be attributed to accumulation of pyroxene alone because their accumulated clinopyroxenes are not nepheline normative [*Foden and Varne*, 1980; *Foden*, 1983; *Kennedy et al.*, 1990; *Carr and Rose*, 1984; *Thirwall and Graham*, 1984; *Shimizu and Arculus*, 1975; *Arculus*, 1976], and thus mixtures of hypersthene- or quartz-normative liquids and such clinopyroxenes would not be nepheline normative, regardless of their CaO contents. Similarly, dissolution by melt inclusions of clinopyroxenes with compositions in the range observed for phenocrysts in the host lavas, either prior to or during entrapment, cannot contribute to their nepheline-normative character.

[16] Nepheline-normative, high-CaO melt inclusions occur in lavas ranging from relatively rare ankaramites that are also CaO-rich and nepheline normative to more normal hypersthene- or quartz-normative basalts and basaltic andesites with relatively low-CaO (<13 wt %) contents. Compositional and isotopic differences between melts preserved in olivine phenocrysts and their host lavas have been observed previously and in a variety of settings [e.g., *Sobolev and Shimizu*, 1993; *Gurenko and Chaussidon*, 1995; *Nielsen et al.*, 1995; *Clocchiatti et al.*, 1998; *Saal et al.*, 1998; *Shimizu et al.*, 1998]. In these cases, melt inclusions have been interpreted as sampling a range of liquids (reflecting a range of source compositions, extents of melting, and/or melting processes) trapped before mixing and homogenization in magma chambers diluted or averaged them to produce the compositions of erupted lavas. In

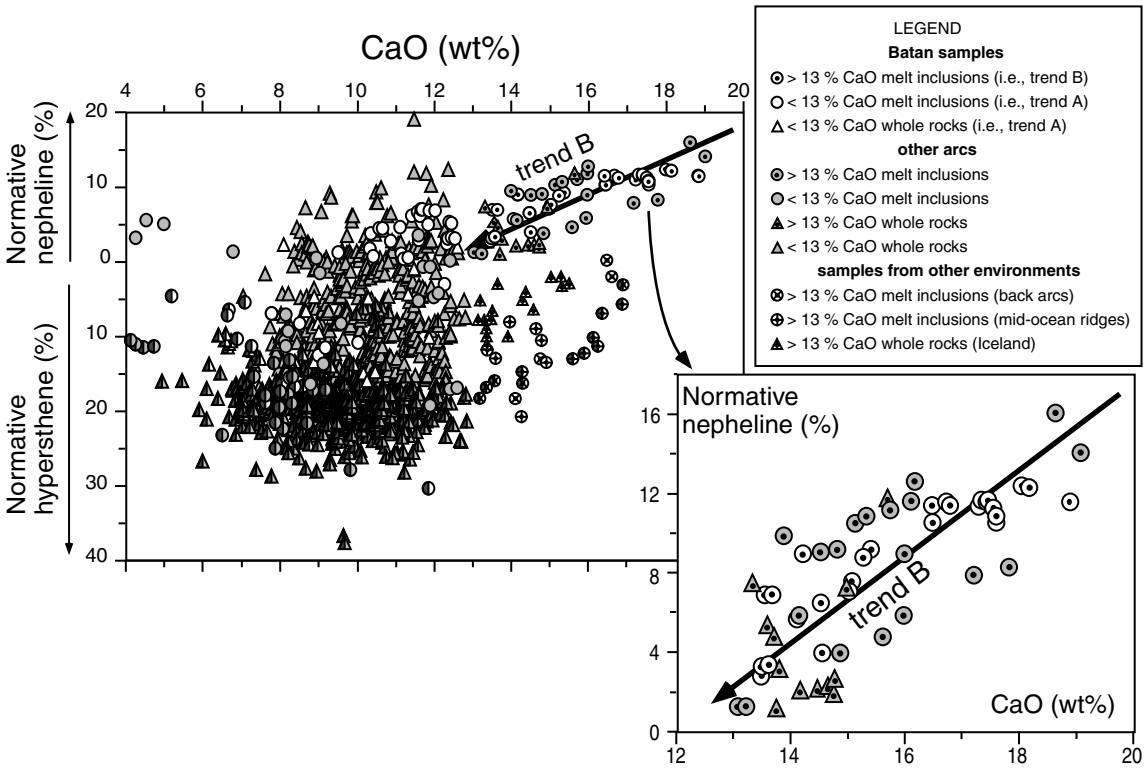

Figure 6. Plot of normative abundances of nepheline and hypersthene versus CaO concentrations comparing Batan CaO-rich melt inclusions (i.e., trend B) and CaO-rich melt inclusions and whole rocks from other arcs (all of which have CaO > 13 wt %) with "normal" melt inclusions and whole rocks from Batan and other arcs (all of which have CaO contents < 13 wt %) (same compilation as in Figure 5). Also shown in this diagram are olivine-hosted CaO-rich melt inclusions from back arc and mid-ocean ridge settings [*Kamenetsky et al*., 1998; *Sours-Page et al*., 1999; *Kamenetsky et al*., 1997] and CaO-rich lavas from Iceland [*Tronnes*, 1990]. Symbols are given in the accompanying legend. Half-solid symbols indicate samples with normative quartz. Major element compositions have been normalized to 100%, and norms were calculated assuming $Fe^{3+} = 0.15 \sum Fe$.

this context, the occurrences of CaO-rich, nepheline-normative melt inclusions in "normal" host lavas and in environments in which whole rocks with comparable compositions have not been identified (Figure 4) demonstrate that the conditions required to produce melts of this sort are more common in subarc environments than might be apparent from the abundance of comparable whole rocks and that such melts contribute more widely to island arc magmatism than their low abundance as erupted magmas might otherwise suggest.

3. Comparison of the Composition of CaO-Rich Melts With Experimental Melts of Iherzolite

[17] The chemical compositions of high-CaO melt inclusions and whole rocks are unusual relative to typical arc magmas and to basaltic

magmas generally, suggesting that production of such magmas requires something other than partial melting of lherzolitic sources. Experimental studies of peridotite melting constrain the range of possible chemical compositions of primary magmas formed over a range of pressures (1 atm to ~100 kbar), degrees of melting (between ~2 and 80%), and bulk compositions of the peridotite sources (plagioclase, spinel, and garnet-bearing peridotites) [*Ito and Kennedy*, 1967; *Mysen and Kushiro*, 1977; *Jaques and Green*, 1980; *Hirose and Kushiro*, 1993; *Baker and Stolper*, 1994; *Kushiro*, 1996; *Walter*, 1998; *Kinzler and Grove*, 1992a, b; *Stolper*, 1980; *Takahashi and Kushiro*, 1983; *Fujii and Scarfe*, 1985; *Falloon and Green*, 1987; *Walter and Presnall*, 1994; *Baker et al.*, 1995; *Kinzler*, 1997; *Wasylenki*, 1998; *Hirose and Kawamoto*, 1995; *Hirose*, 1997a; *Green*, 1973; *Kushiro*, 1972; *Gaetani and Grove*, 1998]. Over this range of variables, CaO concentrations reported for partial melts of dry and hydrous peridotite range from 4 to 14 wt %. When experiments on melting of lherzolite in the presence of CO_2 are included, this range extends to CaO contents >20 wt % [e.g., *Dalton and Presnall*, 1998]. In this section, we briefly review how variations in CaO content (and normative nepheline versus hypersthene) of partial melts of lherzolites relate to changes of pressure, temperature, and source composition (including H_2O and CO_2 content).

[18] Under volatile-free conditions, melts of typical lherzolitic sources can under certain conditions become decreasingly hypersthene normative and even nepheline normative with increasing pressure [*Green and Ringwood*, 1967; *O'Hara*, 1968]; however, they also typically become poorer in CaO, reflecting the decreasing CaO content of clinopyroxene with increasing solidus temperature [e.g., *Longhi*, 1995]. As a result, the effects of pressure alone are unlikely to be capable of extending upward the range of CaO contents of direct melts of lherzolites so as to account for the high CaO content of the magmas in which we are interested or its correlation with normative nepheline. At a given pressure, CaO concentrations (and CaO/Al_2O_3 ratios) in partial melts of lherzolites increase with increasing degree of melting from the solidus and reach a maximum value when clinopyroxene is exhausted from the residue, beyond which further melting leads to decreases in the CaO contents of the partial melts. The maximum CaO contents of liquids produced by volatile-poor experimental melting of fertile lherzolites (~13 wt % [*Jaques and Green*, 1980; *Kinzler and Grove*, 1992b; *Hirose and Kushiro*, 1993; *Baker and Stolper*, 1994; *Kushiro*, 1996; *Walter*, 1998]) thus correspond to the relatively high (up to 25%) degrees of melting typically required for clinopyroxene exhaustion. Although this maximum can increase to 14 wt % CaO at clinopyroxene-out for more depleted peridotites [*Wasylenki*, 1998] (reflecting the low Na_2O contents of the partial melts of depleted peridotites relative to comparable melt fractions of fertile peridotite [*Wasylenki*, 1998; *Hirschmann et al.*, 1998]), it is still well below the CaO contents of the CaO-rich inclusions and lavas identified here. Moreover, liquids produced by the high degrees of melting required to exhaust clinopyroxene from typical lherzolitic sources are not nepheline normative.

[19] *Gaetani and Grove* [1998] showed that increases in the H_2O content of partial melts of lherzolite at constant pressure and decreasing temperature are associated with decreases in the concentrations of SiO_2, FeO, and MgO and with increases in $SiO_2/(MgO + FeO)$ ratios. Consequently, hydrous peridotite melts are SiO_2-rich when compared to anhydrous melts on a volatile-free basis. In addition, melting of lherzolite under hydrous conditions decreases

the CaO concentration of melts at a given melt fraction relative to dry melting [*Hirose and Kawamoto*, 1995; *Hirose*, 1997a]. Consequently, melting of water-bearing lherzolite is not a plausible explanation for the origin of the CaO-rich, silica-undersaturated melts identified here. This is consistent with the observation that CaO-rich, silica-undersaturated olivine-hosted melt inclusions in basalts from Galunggung have low H_2O contents (0.2–0.4 wt %) [*Sisson and Bronto*, 1998].

[20] With the exception of the Lesser Antilles, all the arcs where the CaO-rich melt inclusions and whole rocks have been identified have CO_2-rich sediment subducting [*Plank and Langmuir*, 1998]. Moreover, at pressures above 25 kbar, melting of lherzolite in the presence of CO_2 (or $H_2O + CO_2$, with $X_{CO_2} > 0.5$ [see *Eggler*, 1978]) produces SiO_2-poor liquids with high CaO contents (>20 wt %) and CaO/Al_2O_3 ratios [*Dalton and Presnall*, 1998; *Eggler*, 1978; *Huang and Wyllie*, 1974; *Eggler*, 1974; *Adam*, 1988; *Hirose*, 1997b]. Therefore relatively high pressure melting of carbonated peridotite could play a role in generating the CaO-rich, silica-undersaturated melts identified in this study [*Della-Pasqua and Varne*, 1997]. However, we consider this unlikely based on the significant differences between the CaO-rich, silica-undersaturated arc magmas identified in this study and both experimental melts obtained at high pressures for natural and simple carbonated peridotite systems [*Dalton and Presnall*, 1998; *Hirose*, 1997b] and primitive melilitites, nephelinites, and related rocks from oceanic, continental, and arc regions [*Alibert et al.*, 1983; *Dupuy et al.*, 1989; *Wedephol et al.*, 1994; *Wilson et al.*, 1995; *Maaloe et al.*, 1992; *Hoernle and Schmincke*, 1993; *Clague and Frey*, 1982; *Cheng et al.*, 1993; *Tatsumi et al.*, 1999], which are widely considered to be melts of carbonated peridotite [*Eggler*, 1978; *Huang and Wyllie*, 1974; *Eggler*, 1974; *Adam*, 1988; *Hirose*, 1997b; *Brey and Green*, 1975; *Brey*, 1978; *Wallace and Green*, 1988]. For example, the CaO-rich, silica-undersaturated arc magmas identified here have higher SiO_2 and Al_2O_3 and lower MgO contents at a given CaO content than do the experimental melts obtained at high pressures for natural and simple carbonated peridotite systems (Figure 7). They also show systematic and significant compositional differences from primitive alkali olivine basalts, basanites, olivine nephelinites, and melilitites: that is, although melilitites and nephelinites have CaO contents comparable to those of the inclusions and whole rocks we have studied, the SiO_2 contents of these highly alkalic lavas are typically 5–15 wt % lower than those of the CaO-rich arc magmas. In addition, melilitites and nephelinites (and carbonatites [*Nelson et al.*, 1988]) are characterized by very high concentrations of highly incompatible elements and very high LREE/HREE ratios relative to melt inclusions from B45 sample from Batan (Figure 2b). Finally, CaO-rich, silica-undersaturated melt inclusions and basaltic melt inclusions have similar CO_2 contents (500–750 ppm) in Galunggung basalts [*Sisson and Bronto*, 1998]. Note also that although direct incorporation of carbonate rocks by the primitive arc magmas identified here can account for their elevated CaO contents, it cannot contribute to their nepheline-normative character. Moreover, as Sr and CaO partition strongly into marine carbonates, Sr should accompany any Ca contributed by marine carbonate sediments and carbonate-derived Sr is easily distinguished from mantle-derived Sr by its radiogenic seawater-derived isotopic composition. However, the CaO-rich and CaO-poor lavas from Lombok (Sunda arc), Rindjani (Sunda arc), and Lihir (New Guinea) have undistinguishable $^{87}Sr/^{86}Sr$ ratios [*Foden and Varne*, 1980; *Kennedy et al.*, 1990] and in the case of Grenada (Lesser Antilles), the CaO-rich lavas have lower Sr isotopic ratios than the CaO-poor series [*Hawkesworth et al.*, 1979; *Thirwall and Graham*, 1984]. We therefore conclude that carbonate contribution cannot be

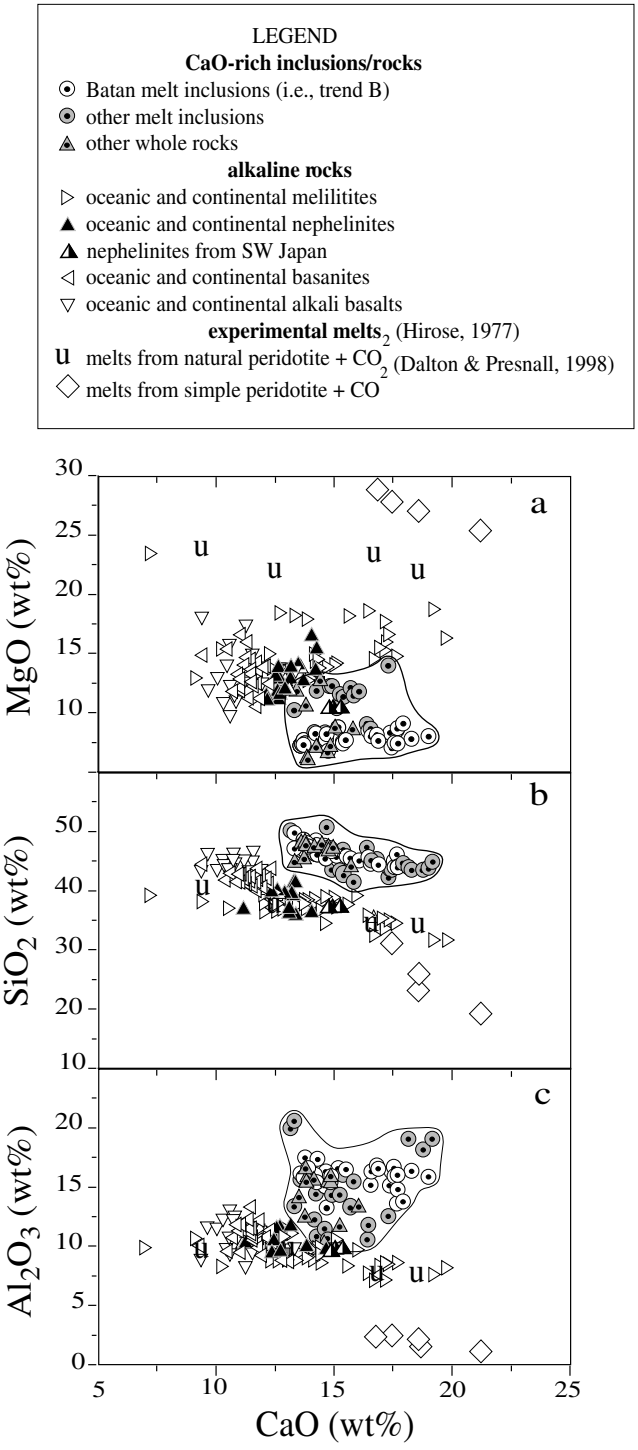
LEGEND
CaO-rich inclusions/rocks
Batan melt inclusions (i.e., trend B)
other melt inclusions
other whole rocks
alkaline rocks
oceanic and continental melilitites
oceanic and continental nephelinites
nephelinites from SW Japan
oceanic and continental basanites
oceanic and continental alkali basalts
experimental melts2 (Hirose, 1977)
melts from natural peridotite + CO2 (Dalton & Presnall, 1998)
melts from simple peridotite + CO
a
b
c
MgO (wt%)
SiO2 (wt%)
Al2O3 (wt%)
CaO (wt%)

reconciled with the composition of the CaO-rich melts identified here.

[21] In summary, we are aware of no conditions under which partial melting of peridotite generates melts having CaO contents and other properties comparable to those observed for CaO-rich melts considered in this study. In particular, only melting at high pressures in the presence of significant CO_2 appears capable of producing liquids with the required CaO contents, but such liquids are significantly different from the CaO-rich arc melts in nearly all other compositional characteristics. In section 4, we develop the hypothesis that the presence of CaO-rich, silica-undersaturated melts similar to the primitive end member of trend B (as defined by the Batan melt inclusions) in arc environments results from the partial melting of clinopyroxene-rich lithologies (e.g., eclogites and/or pyroxenites).

4. Possible Origin of the CaO-Rich, Silica-Undersaturated Arc Melts As Melts of Pyroxene-Rich Sources

[22] In recent years, there have been many suggestions that melting of mafic, pyroxene-rich lithologies may play a significant role in the petrogenesis of basaltic magmas [*Allègre and Turcotte*, 1986; *Hirschmann and Stolper*, 1996; *Hauri*, 1996; *Sigmarsson et al.*, 1998]. Motivations for these suggestions include evidence for heterogeneous sources [*Hanson*, 1977; *Wood*, 1979; *Zindler et al.*, 1984; *Prinzhofer et al.*, 1989] (i.e., melting of a single peridotitic source cannot explain the compositional or isotopic variability of suites of related magmas), the fact that pyroxenites and eclogites are an observed component of mantle and deep, crustal rocks [see *Hirschmann and Stolper*, 1996, and reference therein], and the fact that as the plutonic equivalents of basaltic magmas, they are readily envisioned as a component at depth that can be introduced into other sources as a heterogeneity [e.g., *Allègre and Turcotte*, 1986]. Moreover, subduction of the oceanic crust introduces basaltic components into the mantle, and this provides a plausible mechanism for introducing mafic heterogeneities into largely ultramafic mantle sources. In the context of the high-CaO magmas identified here, an additional reason for thinking about pyroxene-rich source components is that such rocks can have very high CaO contents (see below), and thus high-degree melts of such sources (and perhaps low-degree melts as well) can have CaO contents much higher than melts of peridotite.

[23] In this section, we evaluate in more detail which, if any, naturally occurring pyroxene-rich lithologies are plausible sources of the distinctive magma types identified here. We examine the hypothesis that the primitive CaO-rich, silica-undersaturated magmas identified here reflect partial melting of mafic material by (1) comparison of the major ele-

Figure 7. CaO variation diagrams comparing data for Batan CaO-rich melt inclusions (trend B) and CaO-rich melt inclusions and whole rocks from other arc environments with liquids produced by experiments on natural (lherzolite + 2.5 wt % CO_2 at 30 kbar [*Hirose*, 1997b], solid diamond) and simple (lherzolite-saturated liquids in the CaO-MgO-Al_2O_3-SiO_2-CO_2 system at 60 kbar [*Dalton and Presnall*, 1998], open diamond) carbonated peridotites at high pressure and with primitive (FeO* < MgO in wt %) alkali olivine basalts, basanites, olivine nephelinites, and olivine melilitites from oceanic and continental regions [*Alibert et al.*, 1983; *Dupuy et al.*, 1989; *Wedephol et al.*, 1994; *Wilson et al.*, 1995; *Maaloe et al.*, 1992; *Hoernle and Schmincke*, 1993; *Clague and Frey*, 1982, *Cheng et al.*, 1993]. Also reported are nephelinites from SW Japan [*Tatsumi et al.*, 1999]. Symbols are given in the accompanying legend.

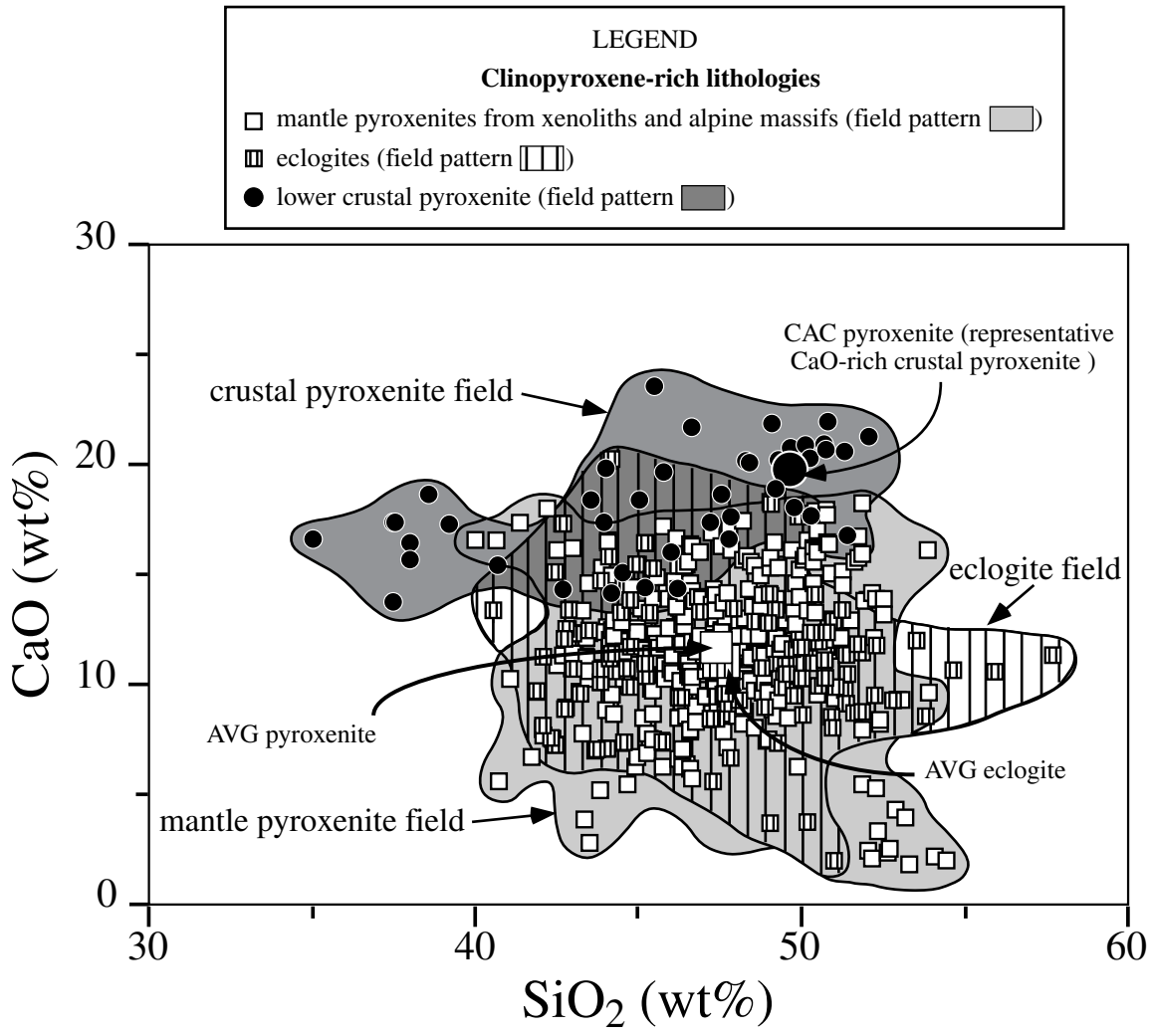

Figure 8. CaO versus SiO_2 concentrations for mantle pyroxenites (open squares) from xenoliths and alpine massifs (compilation by *Hirschmann and Stolper* [1996]), eclogites (dashed squares, compilations from *Hirschmann and Stolper* [1996] and R. L. Rudnick (personal communication, 1999)), and lower crustal pyroxenite cumulates (solid circles) from arc environments [*Irvine*, 1973; *Snoke et al.*, 1981; *Wyllie*, 1967; *Ruckmick and Noble*, 1959; *Findlay*, 1969; *James*, 1971]. Eclogites and pyroxenites were distinguished based on what they were named in the literature. Also shown are the compositions of the average pyroxenite (AVG pyroxenite, corresponding to the mean of the mantle pyroxenite population), average eclogite (AVG eclogite, corresponding to the mean of the eclogite population), and representative CaO-rich crustal pyroxenite (CAC pyroxenite, from Duke Island [*Irvine*, 1973]) used in the MELTS calculations (Figures 9 and 10).

ment compositions of the arc-derived CaO-rich inclusions and whole rocks with model compositions of partial melts of pyroxenite and eclogite calculated using the MELTS algorithm [*Ghiorso*, 1994; *Ghiorso and Sack*, 1995] and (2) comparison of the trace element compositions of the arc-derived CaO-rich samples with the expected trace element compositions of

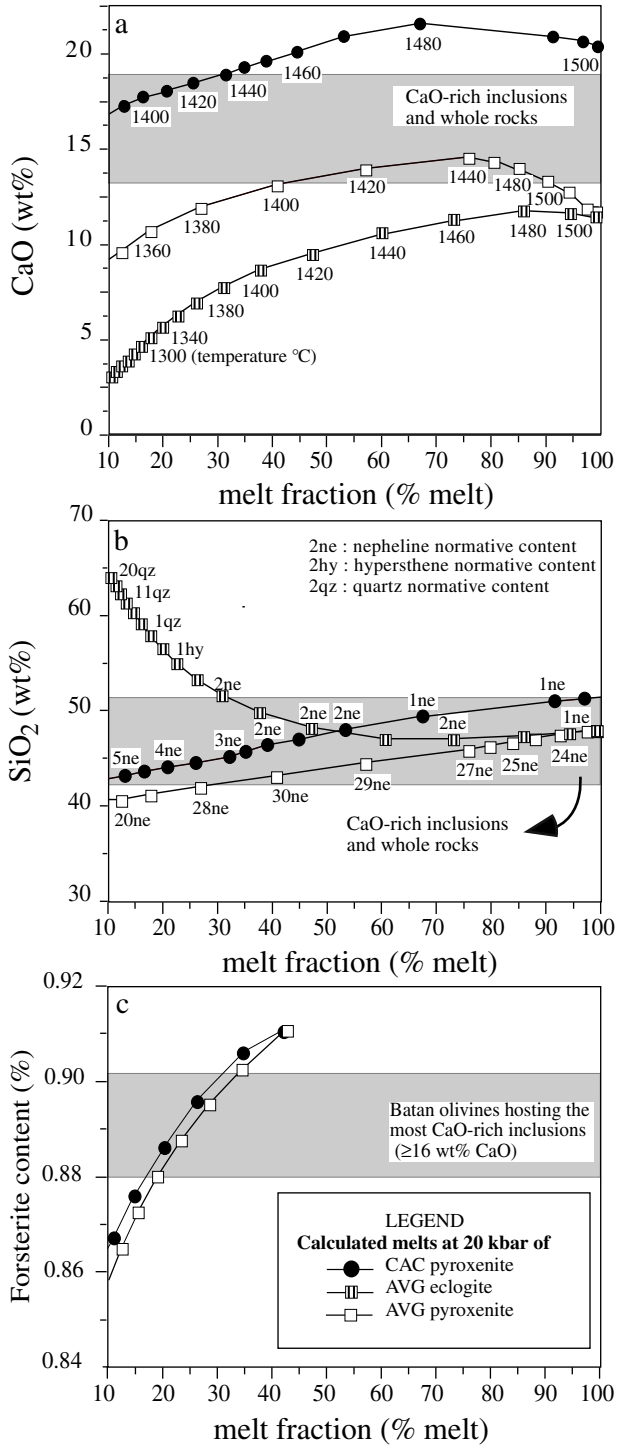
a
CaO (wt%)
melt fraction (% melt)
CaO-rich inclusions
and whole rocks
1300 (temperature °C)
b
SiO2 (wt%)
melt fraction (% melt)
2ne : nepheline normative content
2hy : hypersthene normative content
2qz : quartz normative content
CaO-rich inclusions
and whole rocks
c
Forsterite content (%)
melt fraction (% melt)
Batan olivines hosting the
most CaO-rich inclusions
(≥16 wt% CaO)
LEGEND
Calculated melts at 20 kbar of
CAC pyroxenite
AVG eclogite
AVG pyroxenite

melts of model mantle peridotite, eclogite, and pyroxenite.

4.1 Model Major Element Compositions of Partial Melts of Pyroxenite and Eclogite

[24] Although MELTS is not likely to predict accurately the melting relations of pyroxenites, we, nevertheless, use it as a guide to what to expect because there is such a wide range of pyroxenite and eclogite compositions (Figure 8) and such a small number of melting experiments on such rocks. We acknowledge, however, that the results of these MELTS calculations are at best only semiquantitative at this point and that they must be interpreted cautiously. As shown in Figure 9, MELTS-calculated CaO contents of partial melts of average pyroxenite and eclogite at 20 kbar increase from values at the solidus lower than the concentration in the source to a maximum higher than the concentration in the source, then decrease to the concentration in the source when the liquidus is reached; the maximum in predicted CaO content occurs at very high degrees of melting. This predicted behavior is typical of the pyroxenite and eclogite bulk compositions shown in Figure 8, and it is also predicted for the most CaO-rich pyroxenites (e.g., the representative crustal pyroxenite composition from Duke Island shown in Figure 8). Note that the maximum CaO contents of liquids produced by melting of average mantle pyroxenite and eclogite are, however, still below the CaO contents of the most CaO-rich inclusions and lavas identified in this study, and, in particular, they are lower than the CaO-rich end of trend B defined for the Batan samples. Therefore, according to MELTS, in order to generate melts with CaO contents as high as those required by the most CaO-rich inclusions and lavas at melt fractions of several tens of percent or less, the mafic source would have to be CaO-rich. An important aspect of the MELTS calculations is that even though the average pyroxenite and eclogite sources have similar CaO and SiO_2 contents (Figure 8), melts of average pyroxenite are predicted to have significantly higher CaO and lower SiO_2 contents than melts of average eclogite up to high degrees of melting; the predicted divergent behavior of SiO_2 at low melt fractions (i.e., to very high SiO_2 for low degree melts of the average eclogite and to very low SiO_2 for low degree melts of the average pyroxenite) is particularly striking in Figure 9b. It should also be noted that to the degree to which the pyroxenites are similar in compositions to basalts (or even picrites), they have higher Fe^{2+}/Mg ratios than mantle peridotites, and thus the first liquids they produce on partial melting will have higher Fe^{2+}/Mg ratios than liquids that could be produced by melting of peridotites. Therefore olivine that could coexist with the low degree melts of the pyroxenites must have much lower forsterite content than the typical

Figure 9. Concentrations of CaO and SiO_2 in batch partial melts of the anhydrous AVG pyroxenite (open squares), AVG eclogite (dashed squares), and CAC pyroxenite (solid circles), calculated as a function of melt fraction using the MELTS algorithm at 20 kbar [*Ghiorso*, 1994; *Ghiorso and Sack*, 1995]. Numbers on curves in Figure 9a refer to calculated temperatures (degrees Celsius) of melting (corrected for the overestimation of 100°C due to the overprediction of the stability of orthopyroxene relative to olivine, see *Hirschmann et al.* [1998]); numbers on curves in Figure 9b refer to nepheline, hypersthene, and quartz normative contents of the calculated melts. The ranges of CaO and SiO_2 contents for the CaO-rich inclusions and whole rocks defined in this study are shown for comparison. (c) Forsterite content of residual olivine of the MELTS-calculated partial melts of AVG pyroxenite and CAC pyroxenite versus melt fraction at 20 kbar. The range of forsterite contents for Batan olivines hosting the most CaO-rich inclusions (i.e., the end member of Batan trend B) is shown for comparison.

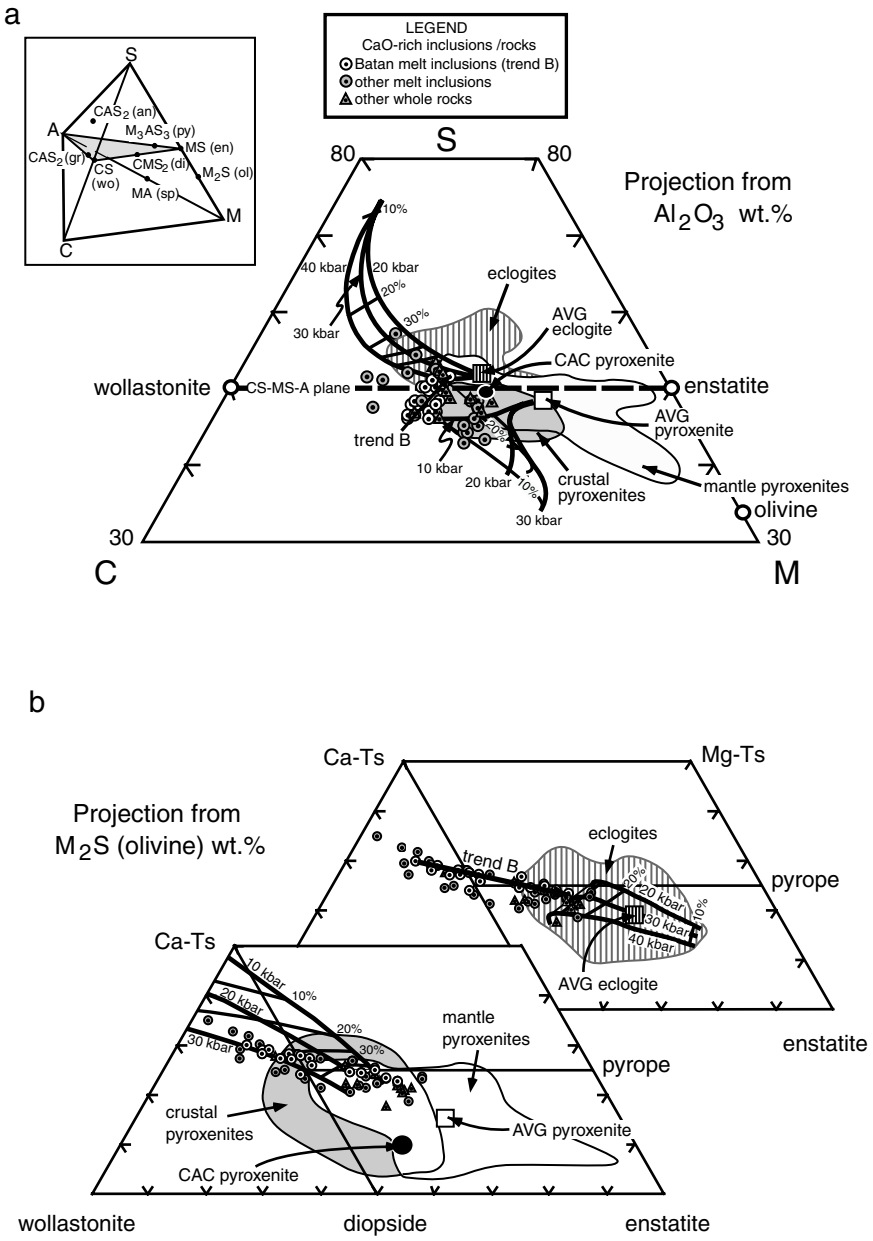

Figure 10. Compositions of CaO-rich melt inclusions from Batan (i.e., trend B) and CaO-rich melt inclusions and whole rocks from other arc environments recalculated to equivalent CaO-MgO-Al_2O_3-SiO_2 (C-M-A-S) and then projected (a) from alumina onto the S-C-M plane and (b) from M_2S (olivine) onto the CS-MS-A (wollastonite-enstatite-alumina) plane. Symbols are given in the accompanying legend. Melting grids calculated using MELTS for AVG pyroxenite (at 10, 20, and 30 kbar) and AVG eclogite (at 20, 30, and 40 kbar), and fields drawn around mantle pyroxenites, eclogites, and lower crustal pyroxenite cumulates (references in caption to Figure 8) are also shown. Figure 10a shows that according to MELTS the CS-MS-A plane is a thermal divide at 10–40 kbar, in agreement with *O'Hara* [1968]: that is, melting (or crystallization) paths of compositions on opposite sides of this plane diverge. (insert) Relationships of planes and projection points in the C-M-A-S system.

Fo_{90} of mantle peridotites. However, the Fe^{2+}/Mg ratio of the partial melts of the pyroxenite will decrease with increasing melt fraction, and thus if the melt fraction is high enough, the forsterite content of the olivine that could crystallize from the partial melts can be as magnesian as Fo_{90} (Figure 9c).

[25] The compositions of partial melts of average eclogite and mantle pyroxenite calculated by MELTS and the compositions of natural CaO-rich, silica-undersaturated melt inclusions and whole rocks have been recast into the C-M-A-S system [*O'Hara*, 1968; *Basaltic Volcanism Study Project*, 1981] and then projected from Al_2O_3 onto the S-C-M plane (Figure 10a) and from M_2S (olivine) onto the CS-MS-A plane (Figure 10b). Figure 10a shows that the average pyroxenite and eclogite compositions are on opposite sides of the CS-MS-A plane. Since this plane is a thermal divide with respect to pyroxene and/or garnet crystallization [*O'Hara*, 1968], melting and crystallization paths of compositions on opposite sides of this plane diverge: Model partial melts of compositions below this plane (i.e., plotting on the silica-poor side of the wollastonite-enstatite join in Figure 10a, as does the average mantle pyroxenite and the representative CaO-rich crustal pyroxenite) produce silica-poor liquids at low degrees of melting, whereas compositions above this plane (i.e., plotting on the silica-rich side of wollastonite-enstatite join in Figure 10a, as does the average eclogite) produce silica-rich liquids at low degrees of melting. The fact that the average eclogite and pyroxenite compositions are on opposite sites of the CS-MS-A thermal divide thus explains the strongly contrasting trends in silica for these two compositions shown in Figure 9b. Note that because the CS-MS-A plane is a thermal divide, partial melts of pyroxene-rich lithologies are confined to one or the other side of this plane, so the fact that the CaO-rich, nepheline-normative melt inclusions (including those defining trend B in Figure 1d) and whole rocks extend across this plane (Figure 10a) confirms our earlier assertion that Batan trend B is not consistent with progressive isobaric melting of pyroxenite, thus leading us to favor a magma mixing origin for this trend. The primitive (i.e., most CaO-rich and nepheline-normative) end of array of CaO-rich magmas plots below the thermal divide, and based on the MELTS calculations, liquids grossly similar to this end of the array could be generated by partial melting of the average mantle pyroxenite (Figures 9 and 10). However, although MELTS calculations based on the average pyroxenite composition can just barely produce partial melts with CaO contents as high as those in trend B (Figure 9a), natural pyroxenites vary substantially in composition, and partial melts similar in CaO content to natural CaO-rich melts considered in this study and in equilibrium with Mg-rich olivine (Figures 9a and 9c) could be generated by intermediate to high degrees of partial melting of a specific subset of natural CaO-rich pyroxenites (lower crustal pyroxenite cumulates such as the representative Duke Island pyroxenite; see section 4.3) at a few tens of kilobars. Moreover, MELTS calculations shows that the FeO contents in the partial melts of pyroxenites are strongly dependent on pressure; i.e., higher FeO melts are produced at higher pressure. Therefore the low FeO content of the CaO-rich, silica-undersaturated melt inclusions and whole rocks relative to "normal" island arc lavas (Figure 5) could reflect their relatively low pressure of formation. When recast into the C-M-A-S system and projected onto the planes of Figure 10, melts of the representative CaO-rich crustal pyroxenite composition shown in Figures 8 and 9 produce at a given pressure liquids similar to the end of the trend B array at lower melt fractions (10–30%) than the average mantle pyroxenite. It should also be noted that most eclogites plot on the silica-rich side of the thermal divide in Figure 10a and thus are less suitable than pyr-

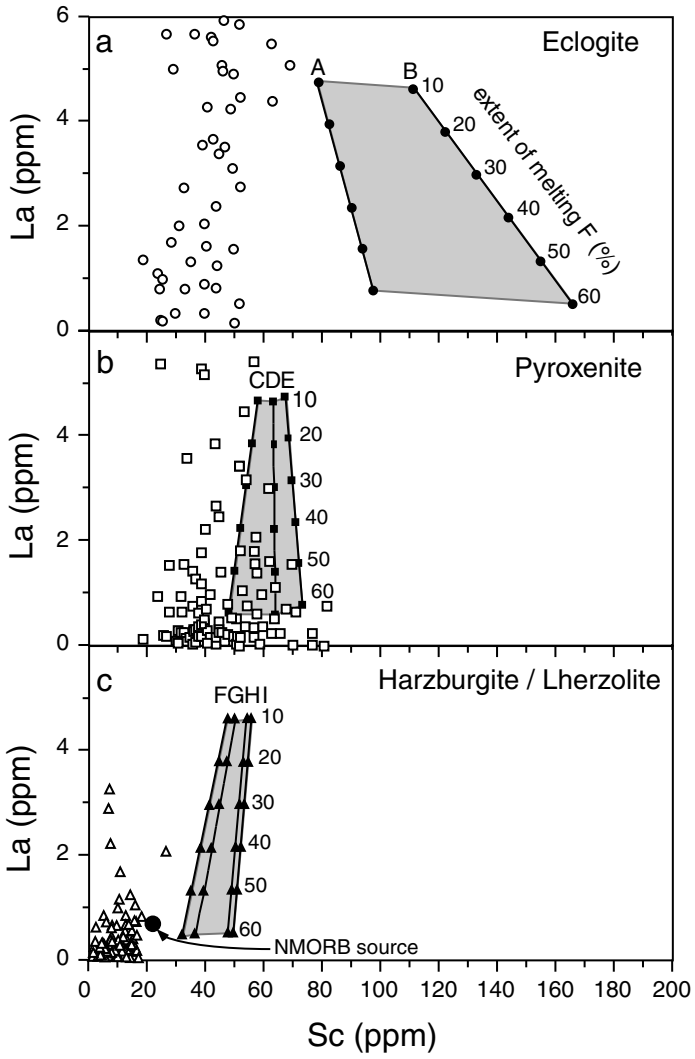

eclogitic residues
- A: 85% cpx and 15 % gt
- B: 25% cpx and 75 % gt

pyroxenitic residues
- C: 40% ol and 60 % cpx
- D: 10% ol, 50% opx and 40% cpx
- E: 85% cpx and 15% sp

natural and synthetic lherzolite residues
- F (KLB-1): 58% ol, 25% opx, 15% cpx and 2% sp
- G (MM3 at 10 kbar): 50% ol, 30% opx, 17% cpx and 3% sp
- H (MM3 at 36 kbar): 56.3% ol, 11.6% opx, 21.4% cpx and 10.7% gt)
- I (DMM1): 64% ol, 27% opx, 7% cpx and 2% sp

oxenites (which typically plot on the silica-poor side of the CS-MS-A plane) as potential sources of CaO-rich, nepheline-normative magmas.

4.2 Trace Element Compositions of Melts of Model Mantle Peridotite, Eclogite, and Pyroxenite

[26] The trace element compositions of liquids at the most CaO-rich, nepheline-normative end of trend B melt inclusions from Batan offer a potential test of the hypothesis that they can be produced by partial melting of pyroxenite. To do this, we have calculated the concentrations of Sc (a typical compatible trace element in clinopyroxene) and La (a typical incompatible trace element) required in the sources of the most CaO-rich melt inclusions from Batan Island, assuming batch melting of those sources, and either pyroxenitic, eclogitic, lherzolitic, or harzburgitic residual assemblages (regardless of major element evidence for or against these possible sources presented above). The measured Sc and La concentrations of the most CaO-rich, nepheline-normative melts are 62 and 8.3 ppm (Table 1; the assumed mineral/melt partition coefficients and residual mineralogies are given in the caption of Figure 11). The calculated compositions of sources consistent with the Sc and La contents of the CaO-rich end of trend B and the Sc and La concentrations of natural mafic and ultramafic rocks [*Bodinier et al*., 1987; *Bodinier*, 1988; *Beard et al*., 1992; *Griffin et al*., 1988; *Gil Ibarguchi et al*., 1989; *Irving*, 1974; *Kurat et al*., 1993; *Pearson et al*., 1993; *Suen and Frey*, 1987; *Taylor and Neal*, 1989; *Van Calsteren*, 1978] are compared in Figure 11. As shown in Figures 11a and 11c, the source compositions required if eclogitic, lherzolitic, or harzburgitic assemblages are assumed are significantly higher in Sc than any naturally occurring mantle eclogites, lherzolites, or harzburgites. In contrast, as shown in Figure 11b, if a pyroxenitic residue is assumed, there is overlap between the required model source compositions and naturally occurring mantle pyroxenites for both Sc and La. These results are consistent with the hypothesis that the

Figure 11. Comparison of the calculated compositions of sources consistent with the Sc and La contents (62 and 8.3 ppm, Table 1) of the most CaO-rich melt inclusions from Batan Island (assuming variable degrees of batch melting of those sources, that the proportions of residual minerals do not change with the degree of melting, and either mafic or ultramafic residual assemblages) with the Sc and La concentrations of natural pyroxenites (open squares), eclogites (open circles), and fertile and depleted lherzolites (open triangles) rocks [*Bodinier et al*., 1987; *Bodinier*, 1988; *Beard et al*., 1992; *Griffin et al*., 1988; *Gil Ibarguchi et al*., 1989; *Irving*, 1974; *Kurat et al*., 1993; *Pearson et al*., 1993; *Suen and Frey*, 1987; *Taylor and Neal*, 1989; *Van Calsteren*, 1978]. Shaded regions represent the ranges of calculated source composition for (a) eclogitic, (b) pyroxenitic, and (c) lherzolitic or harzburgitic residual assemblages, assuming modal phase abundance (given in the accompanying legend) that spans most of the range known in mafic and ultramafic rocks (modal phase abundance for KLB-1 from *Hirose and Kushiro* [1993], MM3 at 10 kbar from *Baker and Stolper* [1994], MM3 at 36 kbar from M. Baker (personal communication), and DMM1 from *Wasylenki* [1998]); the lines in each diagram are the calculated trends of Sc and La concentrations required in these residual assemblages, assuming batch melting of those sources and the numbers along the lines indicate the degree of melting. The concentrations of Sc and La required in the sources were calculated using the general equation of batch melting $C_L = C_0/[D(1 - F) + F]$, where D is the bulk solid/melt partition coefficient weighted by the proportions of the residual solid phases, C_L and C_0 are the concentrations in the liquid and source, respectively, and F is the melt fraction. $D_{\text{solid/melt } i}$ values used in the calculations are for eclogitic, pyroxenitic, and lherzolitic residues assuming the modal phase abundance given in the accompanying legend. Individual mineral melt partition coefficients were compiled from the Geochemical Earth Reference Model (GERM, http://www-ep.es.llnl.gov/germ). Also shown for comparison is the composition of the source of average NMORB estimated by *Hofmann* [1988] based on a crust–upper mantle mass balance.

most CaO-rich, nepheline-normative melts in arc environments are produced by several tens of percent partial melting of pyroxenitic sources and they contribute to evidence against their derivation from melting peridotitic or eclogitic sources.

[27] In summary of this and the previous section, thermodynamic calculations of major element compositions and trace element modeling suggest that the most CaO-rich, nepheline-normative melt inclusions and whole rocks identified in this study are consistent with intermediate to high degree (~10–40 wt %) partial melts of pyroxenites at lower crustal to upper mantle pressures (i.e., up to a few tens of kilobars). If this interpretation is correct, although they are rare as erupted magmas, the widespread geographic occurrence of such melts in arc environments as either melt inclusions or whole rocks would represent previously unrecognized evidence of a widespread contribution to arc magmas of these compositionally distinctive partial melts of mafic material.

4.3. Mantle Pyroxenites Versus Lower Crustal Pyroxenites

[28] MELTS calculations predict that temperatures required to generate CaO-rich melts from anhydrous mantle pyroxenite at 10–30 kbar would be very high (≥1400°C) (Figure 9), a result also supported by preliminary experimental melting of model clinopyroxenites at 10 and 25 kbar [*Hirschmann et al.*, 1995; *Hirschmann and Schiano*, 1999]. Thermal models of arcs [*Davies and Stevenson*, 1992; *Furukawa*, 1993] predict that such high temperatures are present only at 100 km and deeper below the volcanic arc. Such temperatures are also much higher than the homogenization temperatures obtained for the CaO-rich, silica-undersaturated melt inclusions trapped in olivine (typically 1220°–1260°C; see *Metrich et al.* [1999], *Della-Pasqua and Varne* [1997], *Gioncada et al.* [1998], and this study), and although the homogenization temperature is formally only a minimum estimate of the entrapment temperature, these low temperatures are also consistent with equilibrium between trapped melt and the host [*Roedder*, 1984; *Schiano and Bourdon*, 1999; *Lowestern*, 1994; *Student and Bodnar*, 1996].

[29] As we emphasized above, although model melts of pyroxenite are predicted to have CaO concentrations higher than the bulk pyroxenite at high degrees of melting (Figure 9a), the remarkably high CaO contents of the primitive end member of Batan trend B (up to 18–20 wt %) and the existence of a coherent, well-defined high CaO (>14 wt %) group of melt inclusions and whole rocks based on this study would be most easily explained by source compositions characterized by CaO concentrations at the high end of the very large range of CaO contents found in natural pyroxenite. In other words, as shown in Figure 8, mantle-derived pyroxenites are chemically diverse, spanning a range in CaO contents from 18.5 wt % to <5 wt % [*Hirschmann and Stolper*, 1996], and MELTS calculations predict that partial melting of this range of pyroxenites in the upper mantle would generate mostly nepheline-normative melts with similarly variable CaO concentrations, in contrast with the relatively narrow compositional range of CaO-rich, silica-undersaturated melts identified here from eight arcs around the world. Therefore the characteristics of these CaO-rich melts, when combined with the preceding arguments in favor of their derivation from partial melting of pyroxene-rich lithologies on the silica-poor side of the CS-MS-A thermal divide, suggest that they preferentially sample an unusually CaO-rich subset of the full range of naturally occurring pyroxenites.

[30] Clinopyroxene-rich rocks are found in the lower crust beneath exhumed volcanic arcs and

as plutonic xenoliths in arc lavas [*Murray*, 1972; *Irvine*, 1973; *Snoke et al*., 1981; *Conrad and Kay*, 1984; *Kay and Kay*, 1985; *Ducea and Saleeby*, 1996; *DeBari and Coleman*, 1989; *DeBari et al*., 1987]. They occur as zoned ultramafic complexes [see *Wyllie*, 1967, and references therein], typified by the Duke Island ultramafic complex in the Alaskan orogenic belt [*Irvine*, 1973]. These zoned ultramafic complexes have been interpreted as cumulates crystallized from primitive island arc magmas that form layered complexes of hornblende-olivine pyroxenites and less abundant gabbros and diorites [e.g., *Irvine*, 1973; *Snoke et al*., 1981; *Conrad and Kay*, 1984; *Kay and Kay*, 1985; *Ducea and Saleeby*, 1996; *DeBari and Coleman*, 1989; *DeBari et al*., 1987]). The hornblende-olivine pyroxenites in such complexes are characterized by relatively high CaO concentrations (between 13 and 24 wt %), i.e., at the upper end of the range observed for mantle pyroxenites (Figure 8), so melting of these lower crustal lithologies at relatively low pressure to produce the CaO-rich arc magmas (see Figure 9) (rather than the highly variable mantle pyroxenites and eclogites) could thus provide a simple explanation for the restricted, relatively uniform composition of these CaO-rich (and FeO-poor) magmas worldwide. Furthermore, the common presence of amphibole in these pyroxenites would lower their solidus temperatures relative to the anhydrous pyroxenite equivalents we used in the MELTS calculations, therefore at least partially resolving the apparent discrepancy (described at the start of this section) between the inferred temperatures of the CaO-rich, silica-undersaturated melts and the high temperatures required by anhydrous MELTS calculations to produce partial melts of pyroxenites comparable to the trend B compositions. Given the known existence of such cumulates at lower crustal and shallow upper mantle depths beneath arcs [*Ducea and Saleeby*, 1996], their appropriateness as potential sources of CaO-rich, FeO-poor, nepheline-normative melts, and their uniformly high CaO contents relative to mantle pyroxenites, partial melting of lithospheric cumulate pyroxenites rather than of mantle-derived pyroxenites seems to us to be a more plausible explanation for the origin of the distinctive CaO-rich melts considered in this study. The heat source for melting of these lower crustal lithologies could either be trend A arc magmas as they pass through the lower crust or hot ($\geq$ 1320°C [see *Sisson and Bronto*, 1998]), adiabatically upwelled mantle that both produces water-poor arc magmas and heats the overlying lower crust [*Sisson and Bronto*, 1998].

5. Conclusions

[31] 1. Study of major and trace element compositions of olivine-hosted melt inclusions in a high-MgO calc-alkaline basalt from Batan Island (northernmost Philippines, Luzon-Taiwan arc) and of whole rocks (i.e., lavas) from Batan has led to the identification of two populations of magma: (1) A low-CaO (<13 wt %) group defined by melt inclusions in Fo_{85-75} olivines and by Batan whole rocks is referred to as trend A. The compositional trend of these inclusions and whole rocks from Batan is similar to other arc-related lavas, and it is consistent with progressive extraction of olivine + clinopyroxene + amphibole from a parental basaltic liquid with 10 wt % MgO and 45 wt % SiO_2. (2) A CaO-rich (>13 wt %), nepheline-normative group of melt inclusions in Fo_{90-85} olivines is defined as trend B. The compositional trend of these inclusions is interpreted in terms of mixing between the most CaO-rich, nepheline-normative inclusions (i.e., in Fo_{90} olivine) and melts near the most primitive end of trend A defined by more typical island arc magmas.

[32] 2. Primitive island arc magmas characterized by very high CaO contents (up to 19.0 wt %) are present as olivine-hosted melt inclusions and whole rock samples from ten arc volcanoes

from all over the world, including Batan (Luzon-Taiwan arc), Galunggung (Sunda arc), Stromboli and Vulcano (Aeolian arc), Lihir (New Guinea), Nicaragua (Central America), Grenada (Lesser Antilles), Lombok (Sunda arc), Rindjani (Sunda arc), and Epi and Merelava (Vanuatu arc). These CaO-rich magmas define a group that is compositionally distinctive when compared to normal island arc lavas: Not only are they CaO-rich, but they are also nepheline normative and FeO-poor relative to previously recognized primitive arc magmas, and their normative nepheline contents are positively correlated with their CaO content.

[33] 3. The CaO contents of experimental partial melts of fertile or depleted peridotites under dry or hydrous conditions range up to 13–14 wt %: i.e., they are lower than the CaO contents of the CaO-rich, silica-undersaturated arc melts identified in this study. Although melting of peridotite at pressures of a few tens of kilobars in the presence of CO_2 can produce CaO-rich, silica-poor liquids, we consider it unlikely that this is responsible for producing CaO-rich arc-derived melts identified here based on their strong compositional contrasts with the compositions of primitive nephelinites and melilitites and with the compositions of experimental melts of carbonated peridotites.

[34] 4. Thermodynamic calculations of major element compositions (using the MELTS algorithm) and trace element modeling suggest that the most CaO-rich, FeO-poor, nepheline-normative melt inclusions and whole rocks identified in this study could represent intermediate to high degree (~10–40 wt %) partial melts of pyroxenites at lower crustal to upper mantle pressures (up to a few tens of kilobars). However, MELTS calculations predict that temperatures required to generate CaO-rich melts from anhydrous pyroxenite would be $\geq$1400°C, which is high relative to what is required for typical arc magmas. Also, the remarkably high CaO contents of the most CaO-rich inclusions and whole rocks imply a source composition characterized by CaO concentrations at the high end of the range of natural pyroxenites.

[35] 5. Plausible sources of the CaO-rich, silica-undersaturated melts are lower crustal and shallow upper mantle pyroxene-rich cumulates from arc environments because such cumulates have CaO concentrations at the upper end of the range observed in mantle pyroxenites. Moreover, these cumulates often contain amphibole, which would lower their solidus temperatures to values more consistent with those expected in deep crustal or shallow subarc environments.

Acknowledgments

[36] The authors benefited from numerous discussions with M. B. Baker, M. N. Ducea, M. M. Hirschmann, P. Kelemen, R. Maury, N. Metrich, and J. B. Saleeby. M. M. Hirschmann, R. Kessel, T. Plank, and R. L. Rudnick generously made their pyroxenite, eclogite, and arc lava compilations available to us. H. Sato, T. Plank, Y. Tatsumi, and W. M. White provided constructive reviews and comments. Electron microprobe analyses were done at Caltech with assistance from C. Ma. The ion micro-probe analyses were done at the Lawrence Livermore National Laboratory with valuable assistance from D. L. Phinney and I. Hutcheon. Sc analyses were made by I. Hutcheon. This work was supported by NSF grants EAR-9706254 (EMS) and EAR-9805101 (JME) and is Caltech Division of Geological and Planetary Sciences contribution 5709.

References

Adam, J., Dry, hydrous, and CO_2-bearing liquidus phase relationships in the CMAS system at 28 Kb, and their bearing on the origin of alkali basalts, *J. Geol.*, *96*, 709–719, 1988.

Alibert, C., A. Michard, and F. Albarede, The transition from alkali basalts to kimberlites: Isotope and trace element evidence from melilitites, *Contrib. Mineral. Petrol*, *82*, 176–186, 1983.

Allègre, C. J., and D. L. Turcotte, Implications of a two-component marble-cake mantle, *Nature*, *323*, 123–127, 1986.

Arculus, R. J., Geology and geochemistry of the alkali basalt-andesite association of Grenada, Lesser Antilles island arc, *Geol. Soc. Am. Bull.*, *87*, 612–624, 1976.

Armstrong, J. T., Quantitative analysis of silicate and oxide minerals: Comparison of Monte Carlo, ZAF and $\phi(\rho Z)$ procedures, in *Microbeam Analysis*, edited by D. E. Newbury, pp. 239–246, San Francisco Press, San Francisco, Calif., 1988.

Baker, M. B., and E. M. Stolper, Determining the composition of high-pressure mantle melts using diamond aggregates, *Geochim. Cosmochim. Acta*, *58*, 2811–2827, 1994.

Baker, M. B., M. M. Hirschmann, M. S. Ghiorso, and E. M. Stolper, Compositions of near-solidus peridotite melts from experiments and thermodynamic calculations, *Nature*, *375*, 308–311, 1995.

Beard, B. L., L. Medaris, J. Gordon, M. Clark, H. K. Brueckner, and Z. Misar, Petrogenesis of Variscan high-temperature group A eclogites from the Moldanubian Zone of the Bohemian Massif, Czechoslovakia, *Contrib. Mineral. Petrol.*, *111*, 468–483, 1992.

Bodinier, J. L., Geochemistry and petrogenesis of the Lanzo peridotite body, Western Alps, *Tectonophysics*, *149*, 67–88, 1988.

Bodinier, J. L., M. Guiraud, J. Fabries, J. Dostal, and C. Dupuy, Petrogenesis of layered pyroxenites from the Lherz, Freychinede and Prades ultramafic bodies (Ariege, French Pyrenees), *Geochim. Cosmochim. Acta*, *51*, 279–290, 1987.

Brey, G., Origin of Olivine melilitites chemical and experimental constraints, *J. Volcanol. Geotherm. Res.*, *3*, 61–88, 1978.

Brey, G., and D. H. Green, The role of CO_2 in the genesis of olivine melilitite, *Contrib. Mineral. Petrol.*, *49*, 93–103, 1975.

Basaltic Volcanism Study Project, *Basaltic Volcanism on the Terrestial Planets,* Pergamon, New York, 1981.

Carr, M. J., and W. I. Rose, CENTAM: A data base of Central American volcanic rocks, *J. Volcanol. Geotherm. Res.*, *33*, 239–240, 1984.

Cawthorn, R. J., and M. J. O'Hara, Amphibole fractionation in calc-alkaline magma genesis, *Am. J. Sci.*, *276*, 309–329, 1976.

Cheng, Q. C., J. D. MacDougall, and G. W. Lugmair, Geochemical studies of Tahiti, Teahitia and Mehetia, Society island chain. *J. Volcanol. Geotherm. Res.*, *55*, 155–184, 1993.

Clague, D. A., and F. A. Frey, Petrology and trace element geochemistry of the Honolulu volcanics, Oahu: Implication for the oceanic mantle below Hawaii, *J. Petrol.*, *23*, 447–504, 1982.

Clocchiatti, R., P. Schiano, L. Ottolini, and P. Bottazzi, Earlier alkaline and transitional magmatic pulsation of Mt. Etna volcano, *Earth Planet. Sci. Lett.*, *163*, 399–407, 1998.

Conrad, W. K., and R. W. Kay, Ultramafic and mafic inclusions from Adak island: Crystallization history, and implications for the nature of primary magmas and crustal evolution in the Aleutian arc, *J. Petrol.*, *25*, 88–125, 1984.

Dalton, J. A., and D. C. Presnall, The continuum of primary carbonatitic-kimberlitic melt compositions in equilibrium with lherzolite: Data from the system CaO-MgO-Al_2O_3-SiO_2-CO_2 at 6GPa, *J. Petrol.*, *39*, 1953–1964, 1998.

Davidson, J. P., Crustal contamination versus subduction zone enrichment: Examples from the Lesser Antilles and implications for mantle source compositions of island arc volcanic rocks, *Geochim. Cosmochim. Acta*, *51*, 2185–2198, 1987.

Davies, J. H., and D. J. Stevenson, Physical model of source region of subduction zone volcanics, *J. Geophys. Res.*, *97*, 2037–2070, 1992.

DeBari, S. M., and R. G. Coleman, Examination of the deep levels of an island arc: Evidence from the Tonsina ultramafic-mafic assemblage, Tonsina, Alaska, *J. Geophys. Res.*, *94*, 4373–4391, 1989.

DeBari, S., S. M. Kay, and R. W. Kay, Ultramafic xenoliths from Adagdak volcano, Adak, Aleutian Islands, Alaska: Deformed igneous cumulates from the Moho of an island arc, *J. Geol.*, *95*, 329–341, 1987.

Defant, M. J., and M. S. Drummond, Derivation of some modern arc magmas by melting of young subducted lithosphere, *Nature*, *347*, 662–665, 1990.

Della-Pasqua, F. N., and R. Varne, Primitive ankaramitic magmas in volcanic arcs: A melt inclusion approach, *Can. Mineral.*, *35*, 291–312, 1997.

Drummond, M. S., and M. J. Defant, A model for trondhjemite-tonalite-dacite genesis and crustal growth via slab melting: Archean to modern comparisons, *J. Geophys. Res.*, *95*, 21,503–21,521, 1990.

Ducea, M. N., and J. B. Saleeby, Buoyancy sources for a large, unrooted mountain range, the Sierra Nevada, California: Evidence from xenolith thermobarometry, *J. Geophys. Res.*, *101*, 8229–8244, 1996.

Dupuy, C., H. G. Barczus, J. Dostal, P. Vidal, and J. M. Liotard, Subducted and recycled lithosphere as the mantle sources of ocean island basalts from southern Polynesia, central Pacific, *Chem. Geol.*, *77*, 1–18, 1989.

Eggler, D. H., Effect of CO_2 on the melting of peridotite, *Year Book Carnegie Inst. Washington*, *73*, 215–224, 1974.

Eggler, D. H., The effect of CO_2 upon partial melting of peridotite in the system Na_2O-CaO-Al_2O_3-MgO-SiO_2-CO_2 to 35 kb, with an analysis of melting in a peridotite-H_2O-CO_2 system, *Am. J. Sci.*, *278*, 305–343, 1978.

Ewart, A., W. Bryan, and J. Gill, Mineralogy and geochemistry of the younger volcanic islands of Tonga, S.W. Pacific, *J. Petrol.*, *14*, 429–465, 1973.

Ewart, A., R. N. Brothers, and A. Mateen, Mineralogical and chemical evolution of the Tonga-Kermadec-New Zealand island arc, *J. Volcanol. Geotherm. Res.*, *2*, 205–250, 1977.

Falloon, T. J., and D. H. Green, Anhydrous partial melting of MORB pyrolite and other peridotite compositions at 10 kbar: Implication for the origin of primitive MORB glasses, *Mineral. Petrol.*, *37*, 181–219, 1987.

Falloon, T. J., D. H. Green, C. J. Hatton, and K. L. Harris, Anhydrous partial melting of a fertile and depleted peridotite from 2 to 30 kb and application to basalt petrogenesis, *J. Petrol.*, *29*, 1257–1282, 1988.

Findlay, D. C., Origin of the Tulameen ultramafic-gabbro complex, southern British Columbia, *Can. J. Earth Sci.*, *6*, 399–425, 1969.

Foden, J. D., The petrology of the calcaline lavas of Rindjani volcano, East Sunda Arc: A model for island arc petrogenesis, *J. Petrol.*, *24*, 98–130, 1983.

Foden, J. D., and R. Varne, The petrology and tectonic setting of Quaternary-recent volcanic centres of Lombok and Sumbawa, Sunda Arc, *Chem. Geol.*, *30*, 201–226, 1980.

Fujii, T., and C. M. Scarfe, Composition of liquids coexisting with spinel lherzolite at 10 kbar and the genesis of MORBs, *Contrib. Mineral. Petrol.*, *90*, 18–28, 1985.

Furukawa, Y., Depth of the decoupling plate interface and thermal structure under arcs, *J. Geophys. Res.*, *98* 20,005–20,013, 1993.

Gaetani, G. A., and T. L. Grove, The influence of water on melting of mantle peridotite, *Contrib. Mineral. Petrol.*, *131*, 323–346, 1998.

Ghiorso, M. S., Algorithms for the estimation of phase-stability in heterogeneous thermodynamic systems, *Geochim. Cosmochim. Acta*, *58*, 5489–5501, 1994.

Ghiorso, M. S., and R. O. Sack, Chemical mass-transfer in magmatic processes, 4, A revised and internally consistent thermodynamic model for the interpolation and extrapolation of liquid-solid equilibria in magmatic systems at elevated temperatures and pressures, *Contrib. Mineral. Petrol.*, *119*, 197–212, 1995.

Gil Ibarguchi, J. I., M. Mendia, J. Girardeau, and J. J. Peucat, Petrology of eclogites and clinopyroxene-garnet metabasites from the Cabo Ortegal Complex (northwestern Spain), *Lithos*, *25*, 133–162, 1989.

Gill, J. B., *Orogenic Andesites and Plate Tectonics*, 390 pp., Springer-Verlag, New York, 1981.

Gioncada, A., R. Clocchiatti, A. Sbrana, P. Bottazzi, D. Massare, and L. Ottolini, A study of melt inclusions at Vulcano (Aeolian islands, Italy): Insights on the primitive magmas and on the volcanic feeding system, *Bull. Volcanol.*, *60*, 286–306, 1998.

Green, D. H., Experimental melting studies on a model upper mantle composition at high pressure under water-saturated and water-undersaturated conditions, *Earth Planet. Sci. Lett.*, *19*, 37–53, 1973.

Green, D. H., and A. E. Ringwood, The genesis of basaltic magmas, *Contrib. Mineral. Petrol.*, *15*, 103–190, 1967.

Griffin, W. L., S. Y. O'Reilly, and A. Stabel, Mantle metasomatism beneath western Victoria, Australia, II, Isotopic geochemistry of Cr-diopside lherzolites and Al-augite pyroxenites, *Geochim. Cosmochim. Acta*, *52*, 449–459, 1988.

Grove, T. L., and W. B. Bryan, Fractionation of pyroxene-phyric MORB at low pressure: An experimental study, *Contrib. Mineral. Petrol.*, *84*, 293–309, 1983.

Grove, T. L., D. C. Gerlach, and T. W. Sando, Origin of calc-alkaline series lavas at Medicine Lake volcano by fractionation, assimilation and mixing, *Contrib. Mineral. Petrol.*, *80*, 160–182, 1982.

Gurenko, A. A., and M. Chaussidon, Enriched and depleted primitive melts included in olivine from Icelandic tholeiites: Origin by continuous melting of a single mantle column, *Geochim. Cosmochim. Acta*, *59*, 2905–2917, 1995.

Hanson, G. N., Geochemical evolution of the suboceanic mantle, *J. Geol. Soc. Lond.*, *134*, 235–253, 1977.

Hauri, E. H., Major element variability in the Hawaiian mantle plume, *Nature*, *382*, 415–419, 1996.

Hawkesworth, C. J., R. K. O'Nions, and R. J. Arculus, Nd and Sr isotope geochemistry of island arc volcanics, Grenada, Lesser Antilles, *Earth Planet. Sci. Lett.*, *45*, 237–248, 1979.

Hirose, K., Melting experiments on lherzolite KLB-1 under hydrous conditions and generation of high-magnesian andesitic melts, *Geology*, *25*, 42–44, 1997a.

Hirose K., Partial melt compositions of carbonated peridotite at 3 GPa and role of CO_2 in the alkali-basalt magma generation, *Geophys. Res. Lett., 24,* 2837-2840, 1997b.

Hirose, K., and T. Kawamoto, Hydrous partial melting of lherzolite at 1 GPa: The effect of H_2O on the genesis of basaltic magmas, *Earth Planet. Sci. Lett.*, *133*, 463–473, 1995.

Hirose, K., and I. Kushiro, Partial melting of dry peridotites at high pressure: Determination of compositions of melts segregated from peridotites using aggregates of diamonds, *Earth Planet. Sci. Lett.*, *114*, 477–489, 1993.

Hirschmann, M. M., and P. Schiano, Experimental study of partial melts of clinopyroxenite and the origin of ultra-calcic melt inclusions (abstract), paper presented at 9th Annual International Goldschmidt Conference, Cambridge, Mass., 1999.

Hirschmann, M. M., and E. M. Stolper, A possible role for garnet pyroxenite in the origin of the "garnet signature" in MORB, *Contrib. Mineral. Petrol.*, *124*, 185–208, 1996.

Hirschmann, M. M., M. B. Baker, and E. M. Stolper, Partial melting of mantle pyroxenite (abstract), *Eos Trans. AGU*, *76*(46), Fall Meet. Suppl., F696, 1995.

Hirschmann, M. M., M. S. Ghiorso, L. E. Wasylenki, P. D. Asimow, and E. M. Stolper, Calculation of peridotite partial melting from thermodynamic models of minerals and melts, I, Review of methods and comparison with experiments, *J. Petrol.*, *39*, 1091–1115, 1998.

Hoernle, K., and H. Schmincke, The petrology of the tholeiites through melilite nephelinites on Gran Canaria, Canary islands: Crystal fractionation, accumulation and depth of melting, *J. Petrol.*, *34*, 573–597, 1993.

Hofmann, A. W., Chemical differentiation of the Earth: The relationship between mantle, continental crust, and oceanic crust, *Earth Planet. Sci. Lett.*, *90*, 297–314, 1988.

Huang, W. L., and P. J. Wyllie, Eutectic between wollastonite II and calcite contrasted with thermal barrier in MgO-SiO_2-CO_2 at 30 kilobars, with applications to kimberlite-carbonatite petrogenesis, *Earth Planet. Sci. Lett.*, *24*, 305–310, 1974.

Irvine, T. N., Petrology of the Duke Island ultramafic complex, southeastern Alaska, *Geol. Soc. America Mem.*, *138*, 313–335, 1973.

Irving, A. J., Geochemical and high pressure experimental studies of garnet pyroxenite and pyroxene granulite xenoliths from the Delegate Basaltic Pipes, Australia, *J. Petrol.*, *15*, 1–40, 1974.

Ito, E., and R. J. Stern, Oxygen and strontium isotopic investigations of subduction zone volcanism: The case of the Volcano arc and the Marianas island arc, *Earth Planet. Sci. Lett.*, *76*, 312–320, 1985.

Ito, K., and G. C. Kennedy, Melting and phase relations in a natural peridotite to 40 kilobars, *Am. J. Sci.*, *265*, 519–538, 1967.

James, O. B., Origin and emplacement of the ultramafic rocks of the Emigrant Gap area, California, *J. Petrol.*, *12*, 523–560, 1971.

Jaques, A. L., and D. H. Green, Anhydrous melting of peridotite at 0–15 kbar pressure and the genesis of the tholeiitic basalts, *Contrib. Mineral. Petrol.*, *73*, 287–310, 1980.

Kamenetsky, V. S., A. J. Crawford, S. Eggins, and R. Muhe, Phenocrysts and melt inclusion chemistry of near-axis seamounts, Valu Fa Ridge, Lau Basin: Insight into mantle wedge melting and the addition of subduction components, *Earth Planet. Sci. Lett.*, *151*, 205–223, 1997.

Kamenetsky, V. S., S. M. Eggins, A. J. Crawford, D. H. Green, M. Gasparon, and T. J. Falloon, Calcic melt inclusions in primitive olivine at 43°N: Evidence for melt-rock reaction/melting involving clinopyroxene-rich lithologies during MORB generation, *Earth Planet. Sci. Lett.*, *160*, 115–132, 1998.

Kay, R. W., Aleutian magnesian andesites: Melts from subducted Pacific Ocean crust, *J. Volcanol. Geotherm. Res.*, *4*, 117–132, 1978.

Kay, S. M., and R. W. Kay, Role of crystal cumulates and the oceanic crust in the formation of the lower crust of the Aleutian arc, *Geology*, *13*, 461–464, 1985.

Kennedy, A. K., S. R. Hart, and F. A. Frey, Composition and isotopic constraints on the petrogenesis of alkaline arc lavas: Lihir Island, Papua New Guinea, *J. Geophys. Res.*, *95*, 6929–6942, 1990.

Kinzler, R. J., Melting of mantle peridotite at pressures approaching the spinel to garnet transition: Application to mid-ocean ridge basalt petrogenesis, *J. Geophys. Res.*, *102*, 853–874, 1997.

Kinzler, R. J., and T. L. Grove, Primary magmas of mid-ocean ridge basalts, 1, Experiments and methods, *J. Geophys. Res.*, *97*, 6885–6906, 1992a.

Kinzler, R. J., and T. L. Grove, Primary magmas of mid-ocean ridge basalts, 2, Applications, *J. Geophys. Res.*, *97*, 6907–6926, 1992b.

Kurat, G., H. Palme, A. Embey-Isztin, J. Touret, T. Ntaflos, B. Spettel, F. Brandstatter, C. Palme, G. Dreibus, and M. Prinz, Petrology and geochemistry of peridotites and associated vein rocks of Zabargad Island, Red Sea, Egypt, *Mineral. Petrol.*, *48*, 309–341, 1993.

Kushiro, I., Effect of water on the composition of magmas formed at high pressures, *J. Petrol.*, *13*, 311–334, 1972.

Kushiro, I., Partial melting of a fertile mantle peridotite at high pressures: An experimental study using aggregates of diamond, in *Earth Processes: Reading the Isotopic Code, Geophys. Monogr. Ser.*, vol. 95, edited by A. Basu and S. R. Hart, pp. 109–122, AGU, Washington, D. C., 1996.

Longhi, J., Liquidus equilibria of some primary lunar and terrestrial melts in the garnet stability field, *Geochim. Cosmochim. Acta*, *59*, 2375–2386, 1995.

Lowestern, J. B., Chlorine, fluid immiscibility, and degassing in peralkaline magmas from Pantelleria, Italy, *Am. Mineral.*, *79*, 353–369, 1994.

Maaloe, S., D. James, P. Smedley, S. Peterson, and L. B. Garmann, The Koloa volcanic suite of Kauai, Hawaii, *J. Petrol.*, *33*, 761–784, 1992.

Maury, R. C., M. J. Defant, H. Bellon, D. Jacques, J. L. Joron, F. McDermott, and P. Vidal, Temporal geochemical trends in northern Luzon arc lavas (Philippines): Implications on metasomatic processes in the island arc mantle, *Bull. Soc. Geol. Fr.*, *169*, 69–80, 1998.

McDermott, F., M. J. Defant, C. J. Hawkesworth, R. C. Maury, and J. L. Joron, Isotope and trace element evidence for three component mixing in the genesis of the North Luzon arc lavas (Philippines), *Contrib. Mineral. Petrol.*, *113*, 9–23, 1993.

Metrich, N., and R. Clocchiatti, Sulfur abundance and its speciation in oxidized alkaline melts, *Geochim. Cosmochim. Acta,* 60, 4151-4160, 1996.

Metrich, N., P. Schiano, N. Clocchiatti, and R. Maury, Transfer of sulfur in subduction settings: An example from Batan Island (Luzon volcanic arc, Philippines), *Earth Planet. Sci. Lett.*, *167*, 1–14, 1999.

Murray, C. J., Zoned ultramafic complexes of the Alaskan type: Feeder pipes of andesitic volcanoes, *Mem. Geol. Soc. Am.*, *132*, 313–335, 1972.

Mysen, B. O., and I. Kushiro, Compositional variations of coexisting phases with degree of melting of peridotite in upper mantle, *Am. Min.*, *62*, 843–865, 1977.

Nelson, D. R., A. R. Chivas, B. W. Chappell, and M. T. McCulloch, Geochemical and isotopic systematics in carbonatites and implications for the evolution of ocean-island sources, *Geochim. Cosmochim. Acta*, *52*, 1–17, 1988.

Nicholls, A., and A. E. Ringwood, Effect of water on olivine stability in tholeiites and the production of silica-saturated magmas in the island arc environment, *J. Geol.*, *81*, 285–300, 1973.

Nielsen, R. L., J. Crum, R. Bourgeois, K. Hascall, L. M. Forsythe, M. R. Fisk, and D. M. Christie, Melt inclusions in high-An plagioclase from the Gorda Ridge: An example of the local diversity of MORB parent magmas, *Contrib. Mineral. Petrol., 122,* 34-50, 1995.

Nohda, S., and G. J. Wasserburg, Nd and Sr isotopic study of volcanic rocks from Japan, *Earth Planet. Sci. Lett.*, *52*, 265–276, 1981.

O'Hara, M. J., The bearing of phase equilibria studies in synthetic and natural systems on the origin and evolution of basic and ultrabasic rocks, *Earth Sci. Rev.*, *4*, 60–133, 1968.

Pearce, N. J. G., W. T. Perkins, J. A. Westgate, M. P. Gorton, S. E. Jackson, C. R. Neal, and S. P. Chenery, A compilation of new and published major and trace element data for NIST SRM 610 and 612 certified glass reference materials, *Geostand. Newsl.*, *21*, 115–144, 1997.

Pearson, D. G., G. R. Davies, and P. H. Nixon, Geochemical constraints on the petrogenesis of diamond facies pyroxenites from the Beni Bousera peridotite massif, North Morocco, *J. Petrol.*, *34*, 125–172, 1993.

Pichler, H., and W. Zeil, The Cenozoic rhyolite-andesite association of the Chilean Andes, *Bull. Volcanol.*, *35*, 424–452, 1972.

Plank, T., and C. H. Langmuir, An evaluation of the global variations in the major element chemistry of arc basalts, *Earth Planet. Sci. Lett.*, *90*, 349–370, 1988.

Plank, T., and C. H. Langmuir, The chemical composition of subducting sediment and its consequences for the crust and mantle, *Chem. Geol.*, *145*, 325–394, 1998.

Prinzhofer, A., E. Lewin, and C. Allègre, Stochastic melting of a marble cake mantle: Evidence from local study of the East Pacific Rise at 12°50′N, *Earth Planet. Sci. Lett.*, *92*, 189–206, 1989.

Richard, M., R. Maury, H. Bellon, J. F. Stephan, J. M. Boirat, and A. Calderon, Geology of Mt. Iraya volcano and Batan Island, northern Philippines, *Philippine J. Volcanol.*, *3*, 1–27, 1986.

Roedder, E., Fluid inclusions, in *Fluid Inclusions*, *Rev. Mineral.*, vol. 12, edited by E. Roedder, pp. 1–646, 1984.

Ruckmick, J. C., and J. A. Noble, Origin of the ultramafic complex at Union Bay, southeastern Alaska, *Geol. Soc. Am. Bull., 70,* 981- 1017, 1959.

Ryerson, F. J., and E. B. Watson, Rutile saturation in magmas: Implications for Ti-Nb-Ta depletion in island arc basalts, *Earth Planet. Sci. Lett.*, *86*, 225–239, 1987.

Saal, A. E., S. R. Hart, N. Shimizu, E. H. Hauri, and G. D. Layne, Pb isotopic variability in melt inclusions, *Science*, *282*, 1481–1484, 1998.

Sack, R. O., D. Walker, and I. S. E. Carmichael, Experimental petrology of alkalic lavas: Constraints on cotectics of multiple saturation in natural basic liquids, *Contrib. Mineral. Petrol.*, *96*, 1–23, 1987.

Schiano, P., and B. Bourdon, On the preservation of mantle information in ultramafic nodules: Glass inclusions within minerals versus interstitial glasses, *Earth Planet. Sci. Lett.*, *169*, 173–188, 1999.

Shimizu, N., and R. J. Arculus, Rare earth element concentrations in a suite of basanitoids and alkali olivine basalts from Grenada, Lesser Antilles, *Contrib. Mineral. Petrol*, *50*, 231–240, 1975.

Shimizu N., A. V. Sobolev, and G. D. Layne, In-situ Pb isotope analysis of olivine-hosted melt inclusions from mid-ocean ridges (abstract), *Eos Trans. AGU*, *79*(45), Fall Meet. Suppl., F950, 1998.

Sigmarsson, O., S. Carn, and J. C. Carracedo, Systematics of U-series nuclides in primitive lavas from the 1730-36 eruption on Lanzarote, Canary Islands, and implications for the role of garnet pyroxenites during oceanic basalt formations, *Earth Planet. Sci. Lett.*, *162*, 137–151, 1998.

Sisson, T. W., and S. Bronto, Evidence for pressure-release melting beneath magmatic arcs from basalts at Galunggung, Indonesia, *Nature*, *391*, 883–886, 1998.

Sisson, T. W., and T. L. Grove, Experimental investigations of the role of H_2O in calc-alkaline differentiation

and subduction zone magmatism, *Contrib. Mineral. Petrol.*, *113*, 143–166, 1993.

Sisson, T. W., and G. D. Layne, H_2O in basalt and basaltic andesite glass inclusions from four subduction-related volcanoes, *Earth Planet. Sci. Lett.*, *117*, 619–635, 1993.

Snoke, A. W., J. E. Quick, and H. R. Bowman, Bear Mountain igneous complex, Klamath Mountains, California: An ultrabasic to silicic calc-alkaline suite, *J. Petrol.*, *22*, 501–552, 1981.

Sobolev, A. V., and N. Shimizu, Ultra-depleted primary melt included in an olivine from the Mid-Atlantic Ridge, *Nature*, *363*, 151–154, 1993.

Sobolev, A. V., V. L. Barkusov, V. N. Nevsorov, and A. B. Slutsky, The formation conditions of the high-magnesian olivines from the monominerallic fraction of Luna 24 regolith, *Proc. 11th Lunar Sci. Conf.*, 105–116, 1980.

Sours-Page, R., K. T. M. Johnson, R. L. Nielsen, and J. L. Karsten, Local and regional variation of MORB parent magmas: Evidence from melt inclusions from the Endeavour Segment of the Juan de Fuca Ridge, *Contrib. Mineral. Petrol.*, *134*, 342–363, 1999.

Stolper, E., A phase diagram for mid-ocean ridge basalts: Preliminary results and implications for petrogenesis, *Contrib. Mineral. Petrol.*, *74*, 13–27, 1980.

Stolper, E. M., and S. Newman, The role of water in the petrogenesis of Mariana trough magmas, *Earth Planet. Sci. Lett.*, *121*, 293–325, 1994.

Student, J. J., and R. J. Bodnar, Melt inclusion microthermometry: Petrologic constraints from the H_2O-saturated haplogranite system, *Petrology*, *4*, 310–325, 1996.

Suen, C. J., and F. A. Frey, Origins of the mafic and ultramafic rocks in the Ronda Peridotite, *Earth Planet. Sci. Lett.*, *85*, 183–202, 1987.

Takahashi, E., and I. Kushiro, Melting of a dry peridotite at high pressures and basalt magma genesis, *Am. Mineral.*, *68*, 859–879, 1983.

Tatsumi, Y., D. L. Hamilton, and R. W. Nesbitt, Chemical characteristics of fluid phase released from a subducted lithosphere and origin of arc magmas: Evidence from high-pressure experiments and natural rocks, *J. Volcanol. Geotherm. Res.*, *29*, 293–309, 1986.

Tatsumi, Y., R. Arai, and K. Ishizaka, The petrology of a melilite-olivine nephelinite from Hamada, SW Japan, *J. Petrol.*, *40,* 497–509, 1999.

Taylor, L. A., and C. R. Neal, Eclogites with oceanic crustal and mantle signatures from the Bellsbank Kimberlite, South Africa, Part I, Mineralogy, petrography, and whole rock chemistry, *J. Geol.*, *97*, 551–567, 1989.

Thirwall, M. F., and A. M. Graham, Evolution of high-Ca, high-Sr C-series basalts from Grenada, Lesser Antilles: The effects of intra-crustal contamination, *J. Geol. Soc. London*, *141*, 427–445, 1984.

Tormey, D. R., T. L. Grove, and W. B. Bryan, Experimental petrology of normal MORB near the Kane fracture-zone, 22 degrees-25 degrees N, Mid-Atlantic ridge, *Contrib. Mineral. Petrol.*, *96*, 121–139, 1987.

Tronnes, R. G., Basaltic melt evolution of the Hengill volcanic system, SW Iceland, and evidence for clinopyroxene assimilation in primitive tholeiitic magmas, *J. Geophys. Res.*, *95*, 15,893–15,910, 1990.

Van Calsteren, P. W. C., Geochemistry of the polymetamorphic mafic-ultramafic complex at Cabo Ortegal (NW Spain), *Lithos*, *11*, 61–72, 1978.

Walker, D., T. Shibata, and S. F. DeLong, Abyssal tholeiites from the Oceanographer Fracture Zone II: Phase equilibrium and mixing, *Contrib. Mineral. Petrol.*, *70*, 111–125, 1979.

Wallace, M. E., and D. H. Green, An experimental determination of primary carbonatite magma composition, *Nature*, *335,* 343–346, 1988.

Walter, M. J., and D. C. Presnall, Melting behavior of simplified lherzolite in the system CaO-MgO-AL_2O_3-SiO_2-Na_2O from 7 to 35 kbar, *J. Petrol.*, *35*, 329–359, 1994.

Walter, M. J., Melting of garnet peridotite and the origin of komatiite and depleted lithosphere, *J. Petrol.*, *39*, 29–60, 1998.

Wasylenki, L. E., Partial melting of depleted peridotite in the Earth's upper mantle and implications for generation of mid-ocean ridge basalts, Ph.D. thesis, Calif. Inst. of Technol., Pasadena, 1998.

Wedephol, K. H., E. Gohn, and G. Hartmann, Cenozoic alkali basaltic magmas of western Germany and their products of differentiation, *Contrib. Mineral. Petrol.*, *115*, 253–278, 1994.

Wilson, M., J. M. Rosenbaum, and E. A. Dunworth, Melilitites, partial melts of the thermal boundary layer, *Contrib. Mineral. Petrol.*, *119*, 181–196, 1995.

Wood, D. A., A variably veined suboceanic upper mantle? Genetic significance for mid-ocean ridge basalts from geochemical evidence, *Geology*, *7*, 499–503, 1979.

Wyllie, P. J. (ed.), *Ultramafic and Related Rocks,*John Wiley, New York, 1967.

Zindler, A., H. Staudigel, and R. Batiza, Isotope and trace element geochemistry of young Pacific seamonts: Implications for the scale of upper mantle heterogeneity, *Earth Planet. Sci. Lett.*, *70*, 175–195, 1984.